Journal of Applied Physics

Multipole lattice effects in high refractive index metasurfaces

Cite as: J. Appl. Phys. **129**, 040902 (2021); https://doi.org/10.1063/5.0024274
Submitted: 05 August 2020 • Accepted: 27 December 2020 • Published Online: 27 January 2021

Viktoriia E. Babicheva and Andrey B. Evlyukhin

AIP Publishing

Journal of Applied Physics PERSPECTIVE scitation.org/journal/jap

Multipole lattice effects in high refractive index metasurfaces

Cite as: J. Appl. Phys. **129**, 040902 (2021); doi: 10.1063/5.0024274
Submitted: 5 August 2020 · Accepted: 27 December 2020 ·
Published Online: 27 January 2021

Viktoriia E. Babicheva[1,a)] and Andrey B. Evlyukhin[2,3,b)]

AFFILIATIONS

[1]Department of Electrical and Computer Engineering, University of New Mexico, Albuquerque, New Mexico 87131, USA
[2]Institute of Quantum Optics, Leibniz Universität Hannover, 30167 Hannover, Germany
[3]Moscow Institute of Physics and Technology, 9 Institutsky Lane, Dolgoprudny 141700, Russia

[a)]**Author to whom correspondence should be addressed:** vbb@unm.edu
[b)]**Electronic mail:** a.b.evlyukhin@daad-alumni.de

ABSTRACT

In this Perspective, we outline the recent progress, primary achievements, and further directions in the development of high refractive index nanostructures and metasurfaces. In particular, we review the role of multipole lattice effects in resonant properties of underlying nanostructures and nanophotonic elements in detail. Planar optical designs with efficient light control at the nanoscale can be engineered based on photonic lattices that operate in the translational regime between two and three dimensions. Such transdimensional lattices include 3D-engineered nanoantennas supporting multipole Mie resonances and arranged in the 2D arrays to harness collective effects in the nanostructure. Lattice effects in the periodic nanoparticle arrays have recently attracted a lot of attention as they enable not only spectrally narrow resonant features but also resonance position tuning over a broad range. The recent results indicate that different nanoparticle multipoles not only produce resonant spectral features but are also involved in the cross-multipole coupling, and these effects need to be accounted for in photonic designs. Multipole lattice phenomena provide an effective way to control nanoparticle resonances, facilitate excitation of additional multipoles through a cross-multipole coupling, and enable light localization in planar photonic elements. We review different effects related to the same- and cross-multipole interactions in the arrays. Both infinite and finite arrays, as well as lattices of complex-shape nanoparticles, which allow out-of-plane multipole excitations, are considered.

I. INTRODUCTION

Artificially designed materials, so-called metamaterials or metastructures, are being actively explored and are generating widespread interest within the photonics engineering field. These studies are primarily focused on optimizing metastructure building blocks to address specific functional tasks. For example, it has been proposed to use metastructures to achieve super-resolution imaging, control the polarization and orbital angular momentum of the light beam, realize electromagnetic "invisibility," implement high-bandwidth communication channels, etc. There are two types of metastructures depending on the spatial distribution of their building blocks. When the building blocks are arranged in periodic three-dimensional (3D) lattices, one can obtain the bulk metamaterials that control light propagation within the engineered structure volume. In the case of a building block arrangement in two-dimensional (2D) lattices, one gets surface metastructures (or metasurfaces) that can significantly alter the incident light at a subwavelength scale.

Nanoparticles and their clusters made of metals or dielectrics are often used as building blocks of metastructures. Importantly, these nanoparticles can support resonant optical responses that are defined by the materials involved, the metastructure's geometrical parameters, and spectral range. In the case of metal nanoparticles, collective vibrations of conduction electrons provide resonant interaction with light due to localized plasmon resonance. High refractive index dielectric and semiconductor nanoparticles can support so-called Mie resonances associated with electric and magnetic resonant excitation of the displacement current. Compared to metal nanoparticles, optical losses in dielectric ones can be negligible in some spectral range, which explains the growing interest in

exploring optical properties of dielectric metastructures and their applications in nanophotonics.

Nanoparticle assemblies, such as oligomers and clusters, exhibit a variety of unusual optical properties as they support a broad range of resonances.[1,2] Such nanostructures support strong multipole resonances resulting in a high field concentration within the proximity of or inside the nanostructure and provide more efficient confinement as well as light manipulation at the nanoscale.

Multipole resonances in plasmonic and all-dielectric nanostructures put forth a number of exciting applications and are an important emerging area in nanophotonics and optics.[3] The resonant multipole interplay can cause sharp features in the light reflection and transmission spectra, including so-called Fano resonances,[4] of different nanoparticle structures. These sharp features can be utilized in functional optical elements and metasurfaces where a narrowband response is required. Subwavelength nanophotonic structures can significantly enhance light–matter interaction,[5,6] including nonlinear effects,[7–9] and enable a wide range of applications such as optical nanoantennas,[1] photovoltaic devices,[10,11] scattering-type near-field optical microscopy,[12,13] etc.

Due to electromagnetic coupling between nanoparticles, metasurfaces exhibit important effects associated with excitation of lattice resonances when the array period is comparable to the wavelength of single nanoparticle resonance. These lattice resonances, being sensitive to the lattice parameters (such as periods and type of the elementary cell), can significantly modify the profile of transmission and reflection spectra by additional resonant features resulting in significant field enhancement near the metasurface.[14–22] These effects are used in different applications including sensors,[23] nanolasers,[24] light-harvesting devices,[25,26] modulators,[27] and others.[28] In the case of high refractive index materials, the nanoparticle coupling can be observed for both electric and magnetic resonances.[21,29,30] This coupling results in important optical effects,[31] such as resonant suppression of reflection[32] or transmission,[33,34] the lattice invisibility (anapole) effects,[35] and others.

The entire multipole range of a nanostructure response has attracted attention recently as it brings new opportunities in tailoring and dynamically controlling metasurface properties and photonic elements. Subsequently, different types of interference effects associated with the classical dynamic multipole radiation modes have generated interest.[36] Such interference phenomena enable novel effects and related photonic functionalities with nanoscale light manipulation.[37] One can roughly differentiate the interference effects in two categories: between multipoles from the same family and cross-multipole effects. Furthermore, the resonant excitations of multipoles and their interaction in a lattice offer a lot of possibilities to control the light beams by leveraging diffraction effects.[38]

In this Perspective, we overview the recent progress and achievements in theoretical studies of collective effects in high refractive index metasurfaces and the role of multipole coupling in their resonant properties. We demonstrate how analysis of these processes provides a fundamental understanding of collective optical response, the effect applications in a metasurface, and opportunities for further practical designs. Diffraction phenomena have been a subject of attention for well over a century and have stimulated a lot of research work after reported observations of Wood's anomalies. These studies ultimately resulted in active research in the area of collective phenomena in optical structures[39] even before the interest shifted toward plasmonic effects.

The effect of collective nanoparticle resonances was first introduced in plasmonic arrays and is commonly referred to as plasmonic surface lattice resonances. An extensive review of general properties, a broad variety of enabled functionalities, and applications of plasmonic lattice resonances can be found in the previous publications.[40,41] The nanoparticle interaction and excitation of lattice resonances can be associated with the dipole coupling of multiple particles in the cell.[42]

Here, our primary attention is paid to analytical and semi-analytical multipole approaches applied to analyze nanoparticle lattices. They provide possibilities to obtain information about the roles of multipoles directly. In turn, it can be used as guidance in the realization of collective optical effects in metasurfaces that include nanoparticles with Mie resonances. It is important to note that there are other more general numerical approaches for calculating the frequency band structure of infinite periodic particle arrays and the transmission, reflection, and absorption coefficients of array slabs.[43–45]

Eigenmodes are physical quantities that correspond to poles in the complex frequency plane and give rise to resonances and resonant enhancement of multipoles. In nonspherical particles, an eigenmode can resonantly increase more than one multipole. The study approach based on eigenmodes is an additional important research method for investigations of the single resonators and nanostructures. The methods based on an eigenmode analysis can also be applied for the investigation of optical properties of metasurfaces.[46–48] Moreover, this approach can provide information about multipole effects if one applies the technique of multipole classifications for corresponding eigenmodes.[49]

In this Perspective, we focus on the overview of effects behind the pronounced lattice features, lattices of uncoupled multipoles considered so far (e.g., Refs. 21 and 22), and recently demonstrated multipole coupling in the infinite arrays even under the normal incidence of external light waves.[50–52] We discuss how the processes of electric and magnetic multipoles interplay, cross-multipole coupling, resonance induction, and bianisotropic effects can enrich the field by bringing both in-depth understandings of the optical effects and their possible implementation in real-life devices.

While there are many different ways to outline recent techniques of studying multipole lattice effects in a nanoparticle array, we structure our Perspective as follows. First, we describe a general case of a single nanoscatterer with electric and magnetic multipoles (Subsection II A) and how it can be simplified for a spherical nanoparticle (Subsection II B). Next, we highlight multipole-specific lattice effects for the first four multipoles (electric and magnetic dipoles and quadrupoles) remaining in the approximation of the spherical nanoparticle in the periodic array (Sec. III). Here, we also consider lattice-induced cross-multipole coupling for the nanoparticles with up to a quadrupole response (Subsection III E). Third, we discuss the light scattering control in the nanostructures (Sec. IV), including the resonant lattice Kerker effect and the lattice anapole, that is, invisibility (Sec. IV C). The remainder of the Perspective emphasizes the techniques that have the potential to significantly advance in the nearest future, and we highlight further directions at the end of some sections throughout the Perspective.

We describe the techniques of analysis that include periodic Green functions (Sec. V). In what follows, we overview multipole excitations and coupling in the arrays of finite size (Sec. VI). We also highlight emerging techniques to calculate multipole moments excited in the structure with full-wave numerical simulations, often called multipole decomposition (Sec. VII). Finally, we outline dipole coupling effects in the nanoparticles of complex shapes and show how trapped modes with a high-quality factor can be excited in the array (Sec. VIII). We wrap up this Perspective with the discussion of further possible development in the field (Sec. IX).

II. ELECTRIC AND MAGNETIC MULTIPOLES OF A SINGLE NANOSCATTERER

Before discussing lattice multipole effects, let us briefly outline several important positions relating to the multipole optical response of single nanoparticles (nanoantennas).

A. General case of arbitrary-shaped particles

The external monochromatic electromagnetic field (with frequency ω) acting on a dielectric nanoparticle induces displacement current in its volume, which is characterized by the current density $\mathbf{j}(\mathbf{r}, \omega)$, where $\mathbf{r}$ is the radius-vector of a point inside the nanoparticle. The induced current is a source of second (scattered) waves in the system. In the following text, we omit the monochromatic time dependence $\exp(-i\omega t)$ for compactness.

To get multipole decomposition of the waves scattered by the nanoparticle, one can use the following representation:

$$\mathbf{j}(\mathbf{r}) = \int \mathbf{j}(\mathbf{r}')\delta(\mathbf{r}-\mathbf{r}')d\mathbf{r}', \tag{1}$$

where the Dirac delta-function $\delta(\mathbf{r}-\mathbf{r}')$ is expanded in a Taylor series[53] with respect to $\mathbf{r}'$ around the origin of the Cartesian coordinate system (it is convenient to choose this origin at the scatterer center of mass[54]),

$$\delta(\mathbf{r}-\mathbf{r}') = \delta(\mathbf{r}) - (\mathbf{r}'\cdot\nabla)\delta(\mathbf{r}) + \frac{1}{2}(\mathbf{r}'\cdot\nabla)^2\delta(\mathbf{r}) - \cdots. \tag{2}$$

Here, ∇ is the gradient operator with respect to $\mathbf{r}$. Inserting Eq. (2) into Eq. (1) and using the definitions of corresponding multipole moments, one can write[54]

$$\begin{aligned}\mathbf{j}(\mathbf{r}) = &-i\omega\ \mathbf{p}\delta(\mathbf{r}) + \frac{i\omega}{6}\ \hat{Q}\nabla\delta(\mathbf{r}) + [\nabla\times\mathbf{m}\delta(\mathbf{r})]\\ &-\frac{i\omega}{6}\ \hat{O}(\nabla\nabla\delta(\mathbf{r})) - \frac{1}{2}[\nabla\times\hat{M}\nabla\delta(\mathbf{r})] + \cdots,\end{aligned} \tag{3}$$

where only several first multipole moments are explicitly presented: $\mathbf{p}$ and $\mathbf{m}$ are the vectors of electric dipole (ED) and magnetic dipole (MD) moments, respectively, and $\hat{Q}$, $\hat{M}$, and $\hat{O}$ are the tensors of the electric quadrupole (EQ), magnetic quadrupole (MQ), and electric octupole (EOC) moments, respectively.

Inserting the expansion equation (3) in the expression of the electric field radiated by $\mathbf{j}$, we obtain[1]

$$\mathbf{E}(\mathbf{r}) = i\omega\mu_0\int_{V_s}\hat{G}^{\mathrm{FF}}(\mathbf{r},\mathbf{r}')\mathbf{j}(\mathbf{r}')d\mathbf{r}', \tag{4}$$

where $\hat{G}^{\mathrm{FF}}(\mathbf{r},\mathbf{r}')$ is the far-field approximation of the Green's tensor for the system without the scattering object,[1] μ_0 is the vacuum magnetic constant, and V_s is the scatterer volume; one obtains the corresponding multipole decomposition,[54]

$$\begin{aligned}\mathbf{E}(\mathbf{r}) = \frac{k_0^2 e^{ik_S r}}{4\pi\varepsilon_0 r}\Bigg([\mathbf{n}\times[\mathbf{p}\times\mathbf{n}]] + \frac{1}{c_S}[\mathbf{m}\times\mathbf{n}]\\ + \frac{ik_S}{6}\ [\mathbf{n}\times[\mathbf{n}\times\hat{Q}\mathbf{n}]] + \frac{ik_S}{2c_S}[\mathbf{n}\times(\hat{M}\mathbf{n})]\\ + \frac{k_S^2}{6}[\mathbf{n}\times[\mathbf{n}\times\hat{O}(\mathbf{nn})]] + \cdots\Bigg).\end{aligned} \tag{5}$$

Here, k_0 and k_S are the wave numbers in vacuum and the surrounding medium, respectively, ε_0 is the vacuum dielectric constant, c_S is the light speed in the surrounding medium, and $\mathbf{n} = \mathbf{r}/r$ is the unit vector directed to the observation point.

The number of multipoles correctly describing the scattered (radiated) fields depends on size, shape, illumination conditions, and multipole definitions.[55] If the size of a scatterer is much smaller than the wavelength of the incident waves, already a small number of the lowest-order Cartesian multipoles (dipoles and quadrupoles) obtained in the long-wavelength approximation (LWA)[56,57] provides a required accuracy for calculation of the scattered fields.

For larger scatterers, the number of LWA multipoles providing the same accuracy increases quickly. Therefore, in this case, it is more convenient to use the exact multipole moments obtained from the spherical harmonic expansion.[55,57] Note that, frequently, the LWA multipoles are called the Cartesian multipoles, whereas the exact multipoles are referenced as the spherical ones.[55,57,58] Here, we would like to remind the reader that, in general, the multipole moments depend on the choice of the point of their localization.[59] However, for a homogeneous particle, it is convenient to choose its center of mass. This choice is justified as, in this case, the number of multipoles for providing the required accuracy is minimal.

The Cartesian multipole decomposition of the scattering waves can be obtained from the Taylor expansion of an exponential function.[55] Because this expansion converges for any argument, the Cartesian multipole expansion for a finite-size scatterer also converges. However, for large scatterers, the number of Cartesian multipoles can significantly increase in comparison with the number of spherical multipoles, providing the required accuracy.

Although the discussion of this Perspective is limited to lattice effects and phenomena that appear considering multipoles beyond the ED case, we would like to direct the reader to some literature pieces that include multipole effects in a single nanoparticle. An extensive discussion of multipole excitations and interference effects for a single particle can be found in Ref. 36. A review of unconventional modes and specific excitations, such as toroidal and anapole excitations, in the single nanoparticle can be found in Refs. 60 and 61. The exact spherical multipoles and their different presentations in photonics are discussed in the review.[62] Modal expansion concerning causality, nondivergence, and nonresonant contribution can be found in Ref. 63.

B. Dipole and quadrupole polarizability of homogeneous spheres

The most simple way to calculate multipole moments corresponds to the case of homogeneous spherical nanoparticles. Using the concept of multipole polarizabilities, multipole moments can be written in proportion to the incident electric and magnetic fields and their spatial derivatives. In the case of homogeneous nanoparticles of a spherical shape, their multipole responses are characterized by corresponding scalar polarizabilities, which can be expressed through scattering coefficients of the Mie theory.[64] Details of this method for dipole and quadrupole polarizabilities can be found elsewhere.[21,22,51] Briefly, the exact dipole and quadrupole moments of a spherical particle illuminated by a plane wave with electric **E** and magnetic **H** fields are determined as

$$\mathbf{p} = \alpha_p \mathbf{E}(\mathbf{r}_0), \tag{6}$$

$$\mathbf{m} = \alpha_m \mathbf{H}(\mathbf{r}_0), \tag{7}$$

$$\hat{Q} = \frac{\alpha_Q}{2}[\nabla \mathbf{E}(\mathbf{r}_0) + \mathbf{E}(\mathbf{r}_0)\nabla], \tag{8}$$

$$\hat{M} = \frac{\alpha_M}{2}[\nabla \mathbf{H}(\mathbf{r}_0) + \mathbf{H}(\mathbf{r}_0)\nabla], \tag{9}$$

where $\mathbf{r}_0$ is the position of the particle's center. For tensorial terms, we use the convention to define tensor elements $\nabla\mathbf{F} + \mathbf{F}\nabla$ in a Cartesian coordinate system as

$$(\nabla\mathbf{F} + \mathbf{F}\nabla)_{\beta\gamma} = \frac{\partial F_\gamma}{\partial \beta} + \frac{\partial F_\beta}{\partial \gamma},$$

where **F** is a vector of an electric or a magnetic field, $\beta, \gamma = x, y, z$. The polarizabilities in Eqs. (6)–(9) can be written as

$$\alpha_p = i\frac{6\pi\varepsilon_0\varepsilon_S}{k_S^3}a_1, \quad \alpha_m = i\frac{6\pi}{k_S^3}b_1, \tag{10}$$

$$\alpha_Q = i\frac{120\pi\varepsilon_0\varepsilon_S}{k_S^5}a_2, \quad \alpha_M = i\frac{40\pi}{k_S^5}b_2, \tag{11}$$

where a_1, a_2, b_1, and b_2 are the corresponding scattering coefficients of the Mie theory.[64] In the Mie theory, contributions of all toroidal moments are included in the scattering coefficients a_j and b_j determining the exact spherical multipole moments of the spherical homogeneous particles. Therefore, our theoretical model with spherical particles automatically takes into account the toroidal moments associated with the considered coefficients a_1, b_1, a_2, and b_2. In particular, the coefficient a_1 includes a contribution of the toroidal dipole moment. Definitions and a detailed discussion of the toroidal multipoles can be found elsewhere.[65,66]

In the case of particles with a pure real permittivity value (without absorption of electromagnetic energy), all Mie coefficients in the polarizabilities are equal to 1 at the resonant conditions.[67] Therefore, the resonant values of the polarizabilities in Eq. (10) are purely imaginary,

$$\alpha_p^R = i\frac{6\pi\varepsilon_0\varepsilon_S}{k_S^3}, \quad \alpha_m^R = i\frac{6\pi}{k_S^3}, \tag{12}$$

$$\alpha_Q^R = i\frac{120\pi\varepsilon_0\varepsilon_S}{k_S^5}, \quad \alpha_M^R = i\frac{40\pi}{k_S^5}. \tag{13}$$

Note that the optical resonances of dielectric nanoparticles (nanoantennas) are often called "Mie resonances" regardless of nanoparticle shapes as opposed to plasmonic resonances of their metallic counterparts.

III. MULTIPOLES IN AN INFINITE LATTICE OF SPHERICAL PARTICLES

The transdimensional regime of a photonic lattice by definition relates to in-between dimensionalities (2D and 3D). It combines properties of 3D-engineered nanoantennas with excitation of multipole Mie resonances and 2D arrays facilitating collective effects. In earlier works, collective (or lattice) resonances have been mainly considered in dipole approximation.[14–20] Because of the strong nanoparticle excitations, lattice resonances have been mainly observed in the arrays of metal nanoparticles with surface plasmon resonances, and they are often referred to as "plasmonic" or "surface" lattice resonances.[40] However, as we show below, the resonant features can be found in many other optical structures and do not necessarily require plasmonic particles. High refractive index nanoparticles not only support electric resonant excitations, but also enable a strong magnetic response because of the induced current circulations within the nanoparticles. In this section, we study lattice effects that are specific to particular multipole, and ED, MD, EQ, and MQ multipoles are taken into consideration. These resonances are strong for nanoparticles of semiconductor materials, such as silicon or III–V compounds, and can be effectively controlled by the lattice parameters.

Dipole or quadrupole coupling in one-dimensional chains and two-dimensional nanoparticle arrays results in collective lattice effects and multipole resonances with wavelengths flexibly tuned by the lattice periods. Throughout the work, we consider a normally incident, monochromatic, and x-polarized light wave with field components $[E_x(\mathbf{r}) = E_0 \exp(ik_S z), H_y(\mathbf{r}) = H_0 \exp(ik_S z), 0]$. The incident wave propagates in the medium with refractive index n_S, and medium wave number is $k_S = n_S k_0$, where k_0 is the wavenumber in vacuum related to the free-space wavelength λ_0 as $k_0 = 2\pi/\lambda_0$. Schematics of the array under consideration are shown in Fig. 1. For spherical nanoparticles that are considered here, multipole polarizabilities, such as α_p for ED, α_m for MD, α_Q for EQ, and α_M for MQ, can be calculated from Mie theory coefficients, and the approach is shown above for dipoles and quadrupoles and in Refs. 21, 22, and 51.

A. Electric dipole lattice

In the ED approximation, we consider dipole moments of the nanoparticles having only in-plane components (determined by the polarization of the incident waves). Under normal light

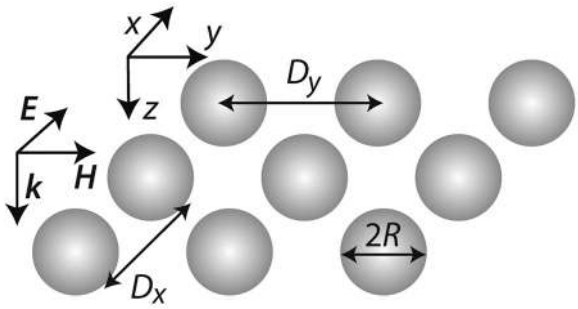

FIG. 1. Rectangular periodic nanoparticle array schematic under consideration. Nanoparticles are surrounded by the uniform medium with the refractive index n_s. Ultra-thin photonic elements and optical nanostructures can be engineered based on transdimensional photonic lattices that include three-dimensional-designed nanoparticles to excite multipole resonances of interest and arranged in two-dimensional arrays to enhance collective effects in the nanostructure.

incidence, each identical spherical nanoparticle arranged in the infinite periodic array has the same ED moment p_0 that is defined by the equation

$$p_0 = \alpha_p E_x + \frac{\alpha_p}{\varepsilon_0} S_{pp} p_0, \tag{14}$$

where α_p is the ED polarizability of the isolated particle, S_{pp} is the sum accounting for the electromagnetic interaction between the EDs arranged into a periodic lattice, and ε_0 is the vacuum permittivity. More details of the derivations can be found in Refs. 15, 21, 22, and 51. The effective polarizability of the particle in the periodic array can be introduced as

$$\alpha_p^{\text{eff}} = \frac{p_0}{E_x} = \left(\frac{1}{\alpha_p} - \frac{S_{pp}}{\varepsilon_0}\right)^{-1}. \tag{15}$$

It exhibits singularity at the wavelength close to the period of the lattice. In particular, for the case of E_x along the x-axis and the wavelength close to Rayleigh anomaly $\lambda \approx \lambda_{\text{RA}-1} = D_y$, the lattice resonances significantly modify the resonance profile of the particles in the array in comparison with a single particle. At the same time, at the wavelength close to another Rayleigh anomaly $\lambda \approx \lambda_{\text{RA}-2} = D_x$, only slight changes of the resonance profile take place. Such behavior is connected with spatial orientation of the particle dipole moments induced by the incident light waves. For the considered example, due to the polarization of the incident wave, the particles in the array have induced ED moments directed along the x-axis. Therefore, the radiation and far-field coupling between the particles is not realized along the x-axis. As a result, the array period D_y (along the y-direction) has the main contribution to the tuning of the lattice resonance.

B. Magnetic dipole lattice

One can show the possibility of the lattice effect for the particles with significant MD resonance, such as silicon nanospheres[21,68,69] and other simple shapes[54,70] or plasmonic core-shell nanoparticles. This effect is a counterpart of the lattice effect based on the ED moment (Fig. 2). The MD moment m_0 of identical particles in the arrays is defined as

$$m_0 = \alpha_m H_y + \alpha_m S_{mm} m_0, \tag{16}$$

where α_m is the MD polarizability of the isolated nanoparticle and S_{mm} is the sum accounting for the electromagnetic interaction between the MDs arranged in the periodic lattice. For more details, see, e.g., Refs. 21 and 51.

Similar to EDs, effective polarizability of the nanoparticle in the lattice can be defined as

$$\alpha_m^{\text{eff}} = \frac{m_0}{H_y} = \left(\frac{1}{\alpha_m} - S_{mm}\right)^{-1}, \tag{17}$$

and lattice resonances of magnetic counterparts can be spectrally tuned and their wavelength is close to the Rayleigh anomaly $\lambda \approx \lambda_{\text{RA}-2} = D_x$. As has been shown in the initial work,[21] the lattice of particles with ED and MD responses can be described by the system of Eqs. (14) and (16), and the electric (magnetic) dipoles can be considered independently from magnetic (electric) counterparts, which is uncoupled. Note that the lattice resonances corresponding to the dipole coupling between nanoparticles are determined by the expressions

$$\text{Re}\frac{1}{\alpha_p^{\text{eff}}} = 0 \tag{18}$$

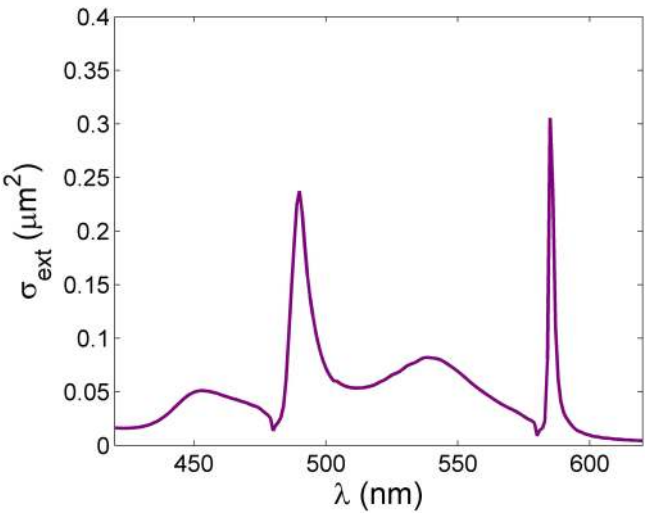

FIG. 2. Extinction cross section per one nanoparticle of infinite Si nanoparticle structures as a function of light wavelength. The narrow peaks at $\lambda = 495$ nm and $\lambda = 590$ nm correspond to the ED and MD lattice resonances, respectively. In the proximity to the Rayleigh anomalies and lattice resonance, the spectral profile has a Fano line shape. The radius of the particles is 65 nm. The nanoparticle array with the rectangular elementary cell 480×580 nm^2 corresponds to the nanoparticle system from Ref. 21.

for ED coupling and

$$\mathrm{Re}\frac{1}{\alpha_m^{\mathrm{eff}}} = 0 \tag{19}$$

for MD coupling.

Two-dimensional periodic arrays of silicon nanoparticles that support lattice resonances due to the ED and MD nanoparticle resonances have been recently analyzed for effects related to collective multipole excitations.[32] Because of the lattice-controlled resonance effects, one can achieve a full overlap between the ED and MD nanoparticle resonances by adjusting lattice periods independently in each mutual-perpendicular direction. What is more important, the strong suppression of light reflection from the nanoparticle array occurs due to destructive interference between the light scattered by EDs and MDs of each nanoparticle in the backward direction with respect to the incident light wave. With this approach, one can realize the resonant lattice Kerker effect,[32] which is resonant suppression of the backward-scattered waves and overall reflection from the array (more details for the realization of this effect are provided in Sec. IV and in Fig. 4). The findings have been supported by an experimental proof of independent resonance control and the observation of a resonant lattice Kerker effect based on the overlap of both ED and MD lattice resonances in silicon cubes.[71]

C. Electric quadrupole lattice

The particles of larger size and/or complex shape support higher multipoles, and lattice resonances are not limited by the dipole approximation. The work[22] has outlined an idea that lattice resonances can be achieved with higher multipole resonances, which provide broader opportunities for control of resonant features in the structures and designing optical elements based on them. Similar to the case of EDs and MDs, it has been shown that the lattice of EDs and EQs can be described by Eqs. (14) and (20), they are excited independently, and they do not couple to their quadrupole or dipole counterpart. In other words, EDs and EQs do not couple to each other in the infinite array of spherical nanoparticles. Similar to the ED array, the EQs can be described by the equation

$$Q_0 = \frac{\alpha_Q i k_S E_x(\mathbf{r}_0)}{2} + \frac{\alpha_Q}{2\varepsilon_0} S_{QQ} Q_0, \tag{20}$$

where α_Q is the EQ polarizability, S_{QQ} is the sum accounting for the electromagnetic interaction between the EQs arranged in the periodic array, and Q_0 is the matrix element in the particle EQ moment $\hat{Q} = Q_0(\hat{x}\hat{z} + \hat{z}\hat{x})$. In the case of EQ, the effective polarizability of the nanoparticle in the lattice is defined as

$$\alpha_Q^{\mathrm{eff}} = \frac{2Q_0}{ik_S E_x} = \left(\frac{1}{\alpha_Q} - \frac{S_{QQ}}{2\varepsilon_0}\right)^{-1}. \tag{21}$$

D. Magnetic quadrupole lattice

In the hypothetical case when the particles in the array have only MQ response, the quadrupole coupling between the particles is described by the equation

$$M_0 = \frac{\alpha_M i k_S H_y}{2} + \frac{\alpha_M}{2} S_{MM} M_0, \tag{22}$$

where α_M is the MQ polarizability, k_S is the wave number in the medium, S_{MM} is the MQ sum accounting for the electromagnetic interaction between the MQ of particles in the array, and M_0 is the matrix element in the particle MQ moment $\hat{M} = M_0(\hat{y}\hat{z} + \hat{z}\hat{y})$. The effective polarizability of the MQ in the lattice is defined as

$$\alpha_M^{\mathrm{eff}} = \frac{2M_0}{ik_S H_y} = \left(\frac{1}{\alpha_M} - \frac{S_{MM}}{2}\right)^{-1}. \tag{23}$$

The lattice resonances corresponding to the quadrupole coupling are determined by the expressions such as Eqs. (18) and (19) written for the quadrupole effective polarizabilities.

Resonant higher-order multipole coupling can be introduced in a similar way. However, as a rule, with increasing particle size, their optical response includes contributions of several first multipoles. Therefore, for the correct description of lattice resonances of the arrays formed by these particles, the coupling models should include all main multipole moments. In this case, cross-multipole effects can be realized.

E. Lattice-induced cross-multipole coupling

The situation of particle interactions can drastically change in the case when the lattice includes simultaneously contributions of several multipoles. It has been shown in Refs. 50 and 51 that the dipole–quadrupole interactions in the infinite lattices can lead to either or both of MD–EQ and ED–MQ coupling effects even at the conditions of the normal light incidence. In these cases, the lattice sums S_{mQ} and S_{Qm} (S_{pM} and S_{Mp}), taking into account MD–EQ (ED–MQ) interactions, are not equal to zero, indicating a cross-multipole coupling of the corresponding dipole and quadrupole moments in the lattices. These multipoles are excited and resonate in response to different fields, for instance, magnetic for MD, MQ, and electric for ED, EQ, and the array facilitates magneto-electric coupling. The equation system describing the dipole and quadrupole moments of the nanoparticle in the lattice and their coupling is the following:

$$\begin{aligned}
p_0 &= \alpha_p E_x(\mathbf{r}_0) + \frac{\alpha_p}{\varepsilon_0}\left[S_{pp} p_0 + \frac{ik_0}{c} S_{pM} M_0\right],\\
m_0 &= \alpha_m H_y(\mathbf{r}_0) + \alpha_m\left[S_{mm} m_0 + \frac{ck_0}{i} S_{mQ} Q_0\right],\\
Q_0 &= \frac{\alpha_Q i k_S E_x(\mathbf{r}_0)}{2} + \frac{\alpha_Q}{2\varepsilon_0}\left[\frac{ik_0}{c} S_{Qm} m_0 + S_{QQ} Q_0\right],\\
M_0 &= \frac{\alpha_M i k_S H_y(\mathbf{r}_0)}{2} + \frac{\alpha_M}{2}\left[\frac{ck_0}{i} S_{Mp} p_0 + S_{MM} M_0\right],
\end{aligned} \tag{24}$$

where the terms with S_{mQ} and S_{Qm} correspond to the MD–EQ cross-multipole coupling in the lattice. Similarly, the terms with S_{pM} and S_{Mp} correspond to ED–MQ cross-multipole coupling. The explicit expressions for the lattice sums can be found in Ref. 51. Based on the

equation system (24), one can derive effective nanoparticle polarizabilities that include cross-multipole coupling,

$$\frac{1}{\alpha_p^{\text{eff, coup}}} = \frac{1 - S_{Mp}\alpha_p^{\text{eff}} \cdot S_{pM}\alpha_M^{\text{eff}} k_0^2/(2\varepsilon_0)}{\alpha_p^{\text{eff}}[1 - S_{pM}\alpha_M^{\text{eff}} k_S^2/2]}, \tag{25}$$

$$\frac{1}{\alpha_m^{\text{eff, coup}}} = \frac{1 - S_{Qm}\alpha_m^{\text{eff}} \cdot S_{mQ}\alpha_Q^{\text{eff}} k_0^2/(2\varepsilon_0)}{\alpha_m^{\text{eff}}[1 + S_{mQ}\alpha_Q^{\text{eff}} k_0^2/(2\varepsilon_0)]}, \tag{26}$$

$$\frac{1}{\alpha_Q^{\text{eff, coup}}} = \frac{1 - S_{Qm}\alpha_m^{\text{eff}} \cdot S_{mQ}\alpha_Q^{\text{eff}} k_0^2/(2\varepsilon_0)}{\alpha_Q^{\text{eff}}[1 + S_{Qm}\alpha_m^{\text{eff}}]}, \tag{27}$$

$$\frac{1}{\alpha_M^{\text{eff, coup}}} = \frac{1 - S_{Mp}\alpha_p^{\text{eff}} \cdot S_{pM}\alpha_M^{\text{eff}} k_0^2/(2\varepsilon_0)}{\alpha_M^{\text{eff}}[1 - S_{Mp}\alpha_p^{\text{eff}}/(\varepsilon_0\varepsilon_S)]}. \tag{28}$$

Note that these complicated expressions are transformed to the more simple ones (15), (17), (21), and (23), respectively, if the coupling effects are neglected.

Some examples of effects on multipole coupling in the lattice are shown in Fig. 3. To include considerable quadrupole effects, we considered silicon nanoparticles of $R = 125$ nm as opposed to smaller ones with $R = 65$ nm in Fig. 4. In the present case, the effective polarizabilities are calculated with Eqs. (15), (17), (21), and (23) for the sphere in the array without cross-multipole coupling $\alpha^{\text{eff}}_{\text{multipole}}$ and Eqs. (25)–(28) taking into account coupling $\alpha^{\text{eff, coup}}_{\text{multipole}}$. Comparing the solid curves (taking into account the coupling effects) with the dashed curves (without the coupling), one can see that the coupling provides strong electromagnetic energy exchange between dipole and quadrupole effective polarizabilities at the conditions of the resonance. For instance, Fig. 3(a) demonstrates strong suppression of an EQ particle response around the wavelength of 820 nm just due to the EQ–MD lattice coupling effect.

F. Lattice sums

As follows from the above text, lattice sums are paramount for calculating the nanoparticles' multipole moments in the arrays and determining the array resonances. Due to their poor convergence, the calculation of these sums requires special attention. There are different techniques for the treatment of this problem, depending on its dimension.[83,84] Using Ewald's method,[85,86] the lattice sums can be converted into two terms converging exponentially. Implementation of this approach can be found, for example, in Refs. 87–90. For the problem of a homogeneous environment, a Fourier modal method has been recently suggested in Ref. 91.

Note that in the spectral regions outside the diffraction bands (outside the Rayleigh anomalies), one can use a simple numerical procedure (with possible next analytical polynomial approximations) for accurate estimation of the lattice sums. For an infinite array, a lattice sum S generally includes infinite number of terms S_n so that

$$S = \lim_{N\to\infty} S_N = \lim_{N\to\infty} \sum_{n=1}^{N} S_n, \tag{29}$$

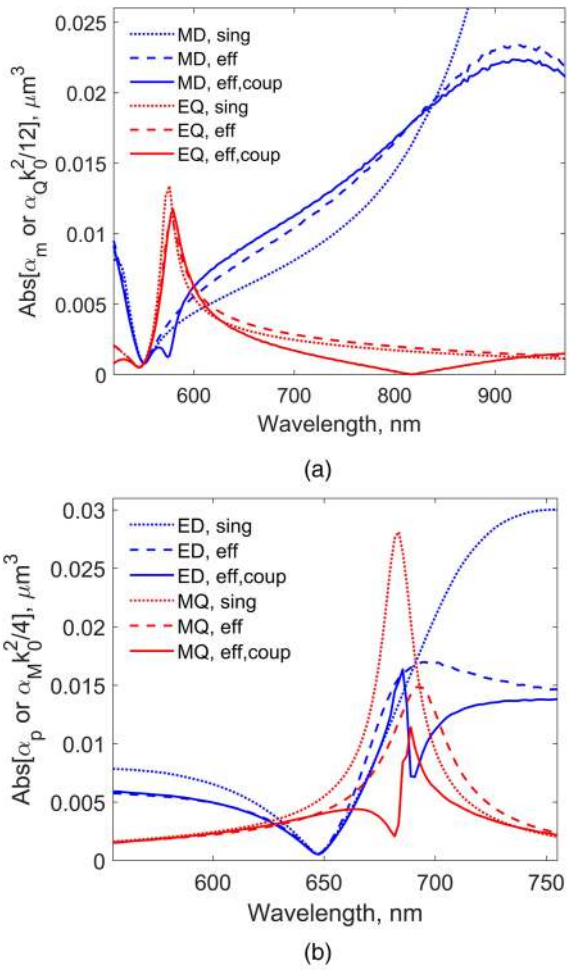

FIG. 3. Comparisons of the multipole nanoparticle resonances in the individual sphere and its periodic array accounting for lattice and cross-multipole coupling: Absolute values of (a) MD and EQ and (b) ED and MQ multipole effective polarizabilities. The figure demonstrates an importance of the cross-multipole coupling between dipole and quadrupole moments of nanoparticles in period arrays. The solid lines in both panels (a) and (b) correspond to the dipole and quadrupole polarizabilities $\alpha^{\text{eff, coup}}$ (denoted "eff, coup") calculated accounting for the cross-multipole coupling effects. One can compare them with other polarizabilities calculated for nanoparticles in free space α (denoted "sing") and in the array neglecting of dipole–quadrupole cross-multipole coupling terms α^{eff} (denoted "eff"). One can see that due to the cross-multipole coupling effect, the excitation of the multipole moments can be suppressed at certain spectral points: (a) EQ(MD) moment is suppressed at the wavelength ~820(670) nm and (b) MQ(ED) moment is suppressed at the wavelength ~680(695) nm. The lattice periods are $D_x = D_y = 285$ nm, and silicon particles have $R = 125$ nm. Effective polarizabilities of MQ and EQ are multiplied by $k_0^2/4$ and $k_0^2/12$, respectively, and effective polarizabilities of ED and EQ are divided by ε_0.

where S_N are the partial sums. For large but finite N, the values of partial sums S_N oscillate around the exact value S for different N. Therefore, using an averaging procedure for a set of different N, one can get an accurate estimate of total S,

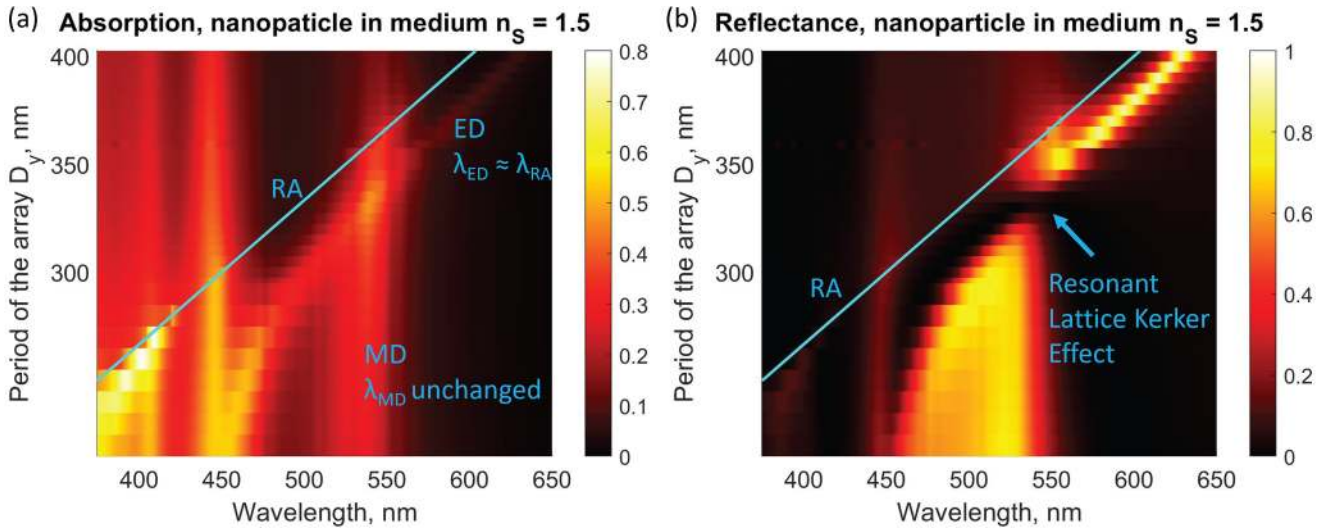

FIG. 4. (a) Absorption and (b) reflection from the array for different periods D_y. The notations "MDR" and "ED-LR" correspond to magnetic dipole and electric dipole lattice resonances, respectively. For the light polarization under consideration, the ED-LR is controlled by D_y. Silicon nanoparticles have $R = 65$ nm, $D_x = 220$ nm, and the surrounding medium is uniform and has refractive index $n_S = 1.5$. Cyan lines "RA" show a wavelength of Rayleigh anomaly. The overlap of ED-LR and MD resonances causes an increase of absorption [panel (a)] and decrease in reflectance [panel (b)] where the resonant lattice Kerker effect is achieved.

$$S \approx S' = \left(\sum_{l=1}^{L} S_{N_l}\right)/L, \tag{30}$$

where L is the number of different N in the set $(N_1, N_2, \ldots, N_L)$ and is considered to be an averaging parameter determined by the required accuracy of the performed estimates. Thus, the developed approach allows us to replace the summation of infinite number terms in (29) by the calculation of several finite-term sums.

In order to get an analytical polynomial presentation of spectral dependence for S, one considers S' as a function of wavelength λ for which the averaging procedure (30) has been realized. Applying the polynomial approximation of $S'(\lambda)$ for the wavelengths from a given spectral range, one determines the coefficients of the polynomial approximation and thus obtains the analytical representation. After that, the obtain polynomial can be used for the simulation of different optical properties of similar types of nanoparticle arrays. Notably, the analytical spectral representations of the lattice sums might significantly simplify the simulations and investigations of lattice resonant effects. Applicability of the suggested procedure is confirmed by the agreement between results obtained using the above approach [Eq. (30)] and full-wave numerical simulations.[51]

Additional information on calculation of poorly converging sums related to lattice resonances can be found elsewhere.[84,89,92,93] For more general approaches of dealing with the periodic arrangements of scatterers and applicable to the structure with an arbitrary number of multipoles, we refer the interested readers to Refs. 43–45 and 94.

IV. APPLICATIONS TO METASURFACES: LATTICE EFFECTS FOR SCATTERING CONTROL

A. Resonant multipole suppression of light transmission (resonant mirror effect)

Now, we demonstrate the case of dipole and quadrupole responses: If dielectric (non-absorbing) particles in periodic infinite arrays support a single multipole lattice resonance, this *always* leads to the total suppression of light transmission at the resonant wavelength for the non-diffracting regime. Note that the non-absorbing regime can be effectively realized with silicon nanoparticles in the infrared spectral range.[95]

Let us start with the dipole approximation for an infinite 2D array of spherical nanoparticles. If the array periodicity is smaller than the operating wavelengths of external, normally incident plane waves, the electric field transmission coefficient t_0 is written as[21]

$$t_0 = 1 + \frac{ik_S}{2S_L}\alpha^{\text{eff}}, \tag{31}$$

where S_L is the area of the array unit cell, α^{eff} is the effective dipole polarizability: $\alpha^{\text{eff}} = \alpha_p^{\text{eff}}/\varepsilon_0\varepsilon_S$ for the ED response, and $\alpha^{\text{eff}} = \alpha_m^{\text{eff}}$ for the MD response. At the resonant conditions, Eqs. (18) and (19) are fulfilled. Thus, from the definitions (15) and (17), we obtain for EDs

$$\frac{1}{\alpha^{\text{eff(R)}}} = i\left(\text{Im}\frac{\varepsilon_0\varepsilon_S}{\alpha_p} - \varepsilon_S \text{Im} S_{pp}\right) \tag{32}$$

and for MDs

$$\frac{1}{\alpha^{\mathrm{eff(R)}}} = i\left(\mathrm{Im}\frac{1}{\alpha_m} - \mathrm{Im}S_{mm}\right). \tag{33}$$

From the ratio between the extinction cross section, which is calculated involving the optical theorem, and the scattering cross section for a lossless ED or MD scatterer,[96] one can obtain the general equation for the imaginary part of $1/\alpha_p$ or $1/\alpha_m$,

$$\mathrm{Im}\frac{\varepsilon_0\varepsilon_S}{\alpha_p} = \mathrm{Im}\frac{1}{\alpha_m} = -\frac{k_S^3}{6\pi}. \tag{34}$$

For the case when the resonant wavelength is larger than the lattice spacing (periodicity) so that all diffracted beams except the zero-order beam are evanescent, the imaginary part of the dipole sums has a simple analytical representation,[97]

$$\varepsilon_S\mathrm{Im}S_{pp} = \mathrm{Im}S_{mm} = \frac{k_S}{2S_L} - \frac{k_S^3}{6\pi}. \tag{35}$$

Inserting Eqs. (34) and (35) into Eqs. (32) and (33), one obtains for the resonant effective polarizability,

$$\alpha^{\mathrm{eff(R)}} = -\frac{2S_L}{ik_S}, \tag{36}$$

and then from Eq. (31) with Eq. (36), we obtain

$$t_0 = 1 + \frac{ik_S}{2S_L}\alpha^{\mathrm{eff(R)}} \equiv 0. \tag{37}$$

Thus, the transmission is totally suppressed at the condition of the ED or MD lattice resonance.

The same result is observed for separate EQ or MQ lattice resonance if we take from Ref. 51 [see also Eq. (44) from Subsection IV B] that

$$t_0 = 1 + \frac{ik_S^3}{8S_L}\alpha^{\mathrm{eff}}_{\mathrm{quadrupole}}, \tag{38}$$

where $\alpha^{\mathrm{eff}}_{\mathrm{quadrupole}} = \alpha^{\mathrm{eff}}_Q/3\varepsilon_0\varepsilon_S$ for the EQs and $\alpha^{\mathrm{eff}}_{\mathrm{quadrupole}} = \alpha^{\mathrm{eff}}_M$ for MQs and also adopt for non-absorbing particles,

$$\mathrm{Im}\frac{3\varepsilon_0\varepsilon_S}{\alpha_Q} = \mathrm{Im}\frac{1}{\alpha_M} = -\frac{k_S^5}{40\pi} \tag{39}$$

and

$$3\varepsilon_S\mathrm{Im}S_{QQ} = \mathrm{Im}S_{MM} = \frac{k_S^3}{4S_L} - \frac{k_S^5}{20\pi}. \tag{40}$$

At the lattice resonant condition

$$\mathrm{Re}\frac{1}{\alpha^{\mathrm{eff}}_{\mathrm{quadrupole}}} = 0, \tag{41}$$

the resonant effective quadrupole polarizability $\alpha^{\mathrm{eff(R)}}_{\mathrm{quadrupole}}$ is

$$\frac{1}{\alpha^{\mathrm{eff(R)}}_{\mathrm{quadrupole}}} = i\left(\mathrm{Im}\frac{1}{\alpha_M} - \frac{S_{MM}}{2}\right) = -\frac{ik_S^3}{8S_L}, \tag{42}$$

that leads to $t_0 = 0$ for t_0 defined by Eq. (38).

Note that similar consideration can be extended to higher-order multipoles. If absorption, even very weak, exists in the system, the transmission coefficient t_0 cannot be equal to 0.

B. Resonant multipole suppression of light reflection (resonant lattice Kerker effect)

1. Single nanoparticle

For a single *dipole* nanoparticle, the first Kerker condition can be formulated as follows:[98] if ED and MD polarizabilities of a nanoparticle [Eq. (10)] satisfy the condition $\alpha_p/\varepsilon_0\varepsilon_p = \alpha_m$, the light scattering from this nanoparticle is suppressed in the backward direction.[99,100] We note that in the original, seminal work,[98] the first Kerker condition for a single nanoparticle is defined through the dual nanoparticle. Nanoparticles with Mie coefficients satisfying $a_n = b_n$ for $n = 1, 2, \ldots$ are called dual nanoparticles as they have electromagnetic duality symmetry. The original work discusses the condition of $\epsilon_{\mathrm{scat}} = \mu_{\mathrm{scat}}$ for the particle material, where ϵ_{scat} and μ_{scat} are the particle's permittivity and permeability, respectively. In engineering terms, it also corresponds to the effective impedance of the scatterer equal to the free-space impedance. However, on further discussion, we always specify the multipole order that the model is limited to, e.g., dipoles, electric quadrupole, both quadrupoles, etc.

At the effect conditions, the strong suppression of light reflectance in the structure appeared due to destructive interference between electromagnetic waves scattered by ED and MD of every nanoparticle in the backward direction with respect to the incident light wave. Recently, this optical phenomenon became to be known as the Kerker effect. For a single silicon spherical nanoparticle array, ED and MD resonances do not overlap, and only non-resonant Kerker effect can be observed.[21,68,69,99–101] Starting with the pioneering work,[102] a number of recent studies suggests that one can achieve a spectral overlap of ED and MD resonances designing all-dielectric nanoparticle shapes and using nanoparticles such as disks, cubes, cones, pyramids, and others.[70,101,103–105] Kerker conditions have been generalized to include scattering waves from different multipoles[106] and achieve directionality control with plasmonic,[107,108] dielectric,[109] or hyperbolic-material scatterers.[81,82]

2. Nanoparticle array

While the single nanoparticle and nanostructure of a finite size are characterized by their scattering, an infinite array of nanoparticles requires introduction of reflection and transmission coefficients. In the case of a dipole–quadrupole system that includes four multipoles and their cross-multipole coupling, the reflection and transmission coefficients, both with respect to an electric field, are

$$r_0 = \frac{ik_S}{2S_L}\left[\frac{1}{\varepsilon_0\varepsilon_S}\alpha_p^{\mathrm{eff/coup}} - \alpha_m^{\mathrm{eff/coup}} - \frac{k_0^2}{12\varepsilon_0}\,\alpha_Q^{\mathrm{eff/coup}} + \frac{k_S^2}{4}\,\alpha_M^{\mathrm{eff/coup}}\right], \tag{43}$$

$$t_0 = 1 + \frac{ik_S}{2S_L}\left[\frac{1}{\varepsilon_0\varepsilon_S}\alpha_p^{\mathrm{eff/coup}} + \alpha_m^{\mathrm{eff/coup}} + \frac{k_0^2}{12\varepsilon_0}\,\alpha_Q^{\mathrm{eff/coup}} + \frac{k_S^2}{4}\,\alpha_M^{\mathrm{eff/coup}}\right]. \tag{44}$$

The expressions of Eqs. (43) and (44) can be obtained from the formulas of the reflection and transmission coefficients presented in Ref. 35 [or Eqs. (51) and (52) here], for the x-polarization, if one writes the multipole moments of spherical nanoparticles through the corresponding polarizabilities.

The concept of Huygens' metasurfaces has been introduced for the case when only substantial ED and MD resonances are excited and compensate each other in the backward scattering (in the analogy of Huygens' source that has zero backscattering).[103,104] Huygens' metasurfaces based on the Kerker effect have a rapid change of the transmitted light phase spanning the whole 2π range. Another full-transparency regime is possible to achieve when all four multipoles are involved and compensate the contributions of each other in the forward- and backward-scattered waves.[35,70] It includes a Kerker-like condition for quadrupoles and an anti-Kerker condition of the dipole–quadrupole scatterers (the coherent dipoles are in a π phase relation with respect to the coherent quadrupoles). This effect is referred to as lattice invisibility. Alternatively, the term "transverse Kerker effect" has also been used as the scattered power is redirected to the lateral direction.[110,111] In what follows, we highlight several examples when lattice-controlled resonances overlap with each other and realize near-zero reflection, in other words, the resonant lattice Kerker effect.

3. ED and MD overlap in silicon array

Collective effects and lattice resonances bring additional mechanisms to control the spectral position of resonances. In particular, even in the case when resonances of the single nanoparticle do not overlap, array periods can be chosen independently in each mutual-perpendicular direction, and it is possible to overlap the ED and MD lattice resonances of nanoparticles in the certain spectral range. As a result, one can realize the resonant lattice Kerker effect, that is, resonant suppression of the backward scattering or reflection.[32] We illustrate the effect of the lattice periodicity on dipole resonance positions in Fig. 4. In particular, the figure shows how the ED lattice resonance (ED-LR) position can be controlled by the period D_y and that the ED-LR overlap with MD resonance (MDR) results in near-zero reflection.[32]

The reflection and transmission coefficients are defined by ED and MD polarizabilities as[21]

$$r_0 = \frac{ik_S}{2S_L}\left[\frac{1}{\varepsilon_0\varepsilon_S}\alpha_p^{\mathrm{eff}} - \alpha_m^{\mathrm{eff}}\right], \tag{45}$$

$$t_0 = 1 + \frac{ik_S}{2S_L}\left[\frac{1}{\varepsilon_0\varepsilon_S}\alpha_p^{\mathrm{eff}} + \alpha_m^{\mathrm{eff}}\right]. \tag{46}$$

From Eq. (45), one can see that the reflectance is totally suppressed when the ED and MD effective polarizabilities are equal to each other. As it has been shown in Subsection IV A, for the case of non-absorbing particles, the effective ED and MD polarizabilities $\alpha^{\mathrm{eff(R)}}$ have the same resonant value of $(i2S_L/k_S)$ [see Eq. (36)]. Therefore, in this case, if the ED and MD moments of the particles in the array reach the resonances at the same wavelength, the reflection goes to zero and the transmission coefficient becomes equal to -1. The minus indicates that the transmitted light has a π phase shift with respect to the incident wave. Such behavior is considered the resonant lattice Kerker effect.

Again, note that for silicon nanoparticles, the electromagnetic absorption is negligibly small in the near-infrared spectral range; therefore, the above theory can be applied to such nanoparticles. If the absorption cannot be neglected, the transmission efficiency cannot reach 100% at the conditions of the resonant lattice Kerker effect.

4. ED and MD overlap in a core-shell nanoparticle array

The recent work has shown that an overlap of MD and ED lattice resonances and a lattice Kerker effect can be achieved not only for the array of silicon nanoparticles, but also for core-shell nanoparticles.[32] In contrast to silicon spherical nanoparticles, where ED and MD resonances are spectrally separated, the second case is for the nanoparticles where MD and ED resonances coincide and are in the near-infrared spectral range with small optical losses. Also, to realize an overlap between MD and ED lattice resonances, it is necessary to take arrays with square elementary cells and with the size being larger than the wavelength corresponding to both MD and ED resonances of an individual particle in the array. In this case, one can see that both lattice resonances can be tuned together, and zero reflectance can be achieved. At the same time, the results demonstrate a very high sensitivity of the lattice Kerker effect to the lattice periodicity because of the narrow resonant increases of dipole sums in the region of the dipole lattice resonances. As a result, only in the narrow spectral region, the effective ED and MD polarizabilities can be equal to each other providing realization of the resonant lattice Kerker effect.

5. Generalized Kerker effect with ED, MD, and EQ overlap[51]

The analysis of multipole resonances in the lattice has shown that even in the case of the homogeneous environment, small nanoparticles with a weak EQ and MD response enable excitation of well-pronounced lattice resonance due to EQ and MD coupling between nanoparticles in the array. Moreover, overlapping EQ and MD resonances with the broad ED response outside its lattice resonance, one can observe a suppression of total reflectance, which is in its generalized form taking into account ED, EQ, and MD, and their coupling in the lattice is defined as

$$r_0 = \frac{ik_S}{2S_L}\left[\frac{1}{\varepsilon_0\varepsilon_S}\alpha_p^{\text{eff}} - \alpha_m^{\text{eff/coup}} - \frac{k_0^2}{12\varepsilon_0}\,\alpha_q^{\text{eff/coup}}\right]. \quad (47)$$

The observed decrease in reflectance is achieved because the Kerker condition of the directional scattering is satisfied. The results of the calculations show that the EQ–MD coupling is critical for correct calculations of the wavelength where the generalized Kerker condition of directional scattering is satisfied. The directional scattering and the Kerker effect appear at the wavelength of strong EQ and MD excitations. The resonant Kerker effect is enabled by destructive interference between the ED resonance of a single particle in the array and the EQ–MD lattice resonance of the particle with the non-resonant contribution of EQ and MD multipoles.

C. Lattice invisibility (anapole)

Recently, using the multipole decomposition approach, the effect of the all-dielectric metasurface invisibility has been demonstrated in metasurfaces formed by the resonant cubic silicon nanoparticles.[35] The effect is explained by simultaneous excitation of both dipole and quadrupole moments in the nanoparticles of the metasurface, which provide, due to interference, simultaneous significant suppression of the forward and backward light scattering. Note that this effect, considered a lattice anapole effect, can be realized in metasurfaces formed by nanoparticles of different shapes and supporting resonant dipole and quadrupole responses. By tuning lattice parameters to, for instance, $D_x = 500$ nm and $D_y = 440$ nm, one can achieve almost total compensation of waves scattered in the forward and backward directions by each multipole (Fig. 5). This results in anapole-like states enabled by the lattice effects.[51] Figure 6 demonstrates the lattice invisibility (anapole) effect in the metasurfaces formed by the spherical silicon nanoparticles.[51]

Finally, we would like to once again mention the similarity and difference between the resonant lattice Kerker effect and lattice invisibility (anapole). In both cases, we aim to design structure with strong interaction of light with matter and to achieve zero reflection and near-unit transmission, as well as leverage collective effects in the nanoparticle array. The main difference is that in the anapole state, the phase of transmitted light almost coincides with the phase of the incident light providing the invisibility effect. In contrast, the resonant Kerker effect resulting in the maximum transmission is accompanied by the phase differences between the incident and transmitted light, spanning the 2π range. These and other scattering effects discussed in the literature so far are summarized in Fig. 7.

As for future directions, we anticipate that more effects based on multipole interplay, interference, and coupling will be discovered and applied to control the optical response of nanoscatterers as building blocks of metasurfaces and photonic elements.

D. Role of coupling

To sum up the above discussion, we once again highlight the optical phenomena that need to be accounted for in the metasurface designs with recently demonstrated effects of same- and cross-multipole coupling.

First of all, the nanoparticle arrangement in a periodic array can significantly enhance the multipole response even in the case when a single nanoparticle has a small, nearly negligible, multipole

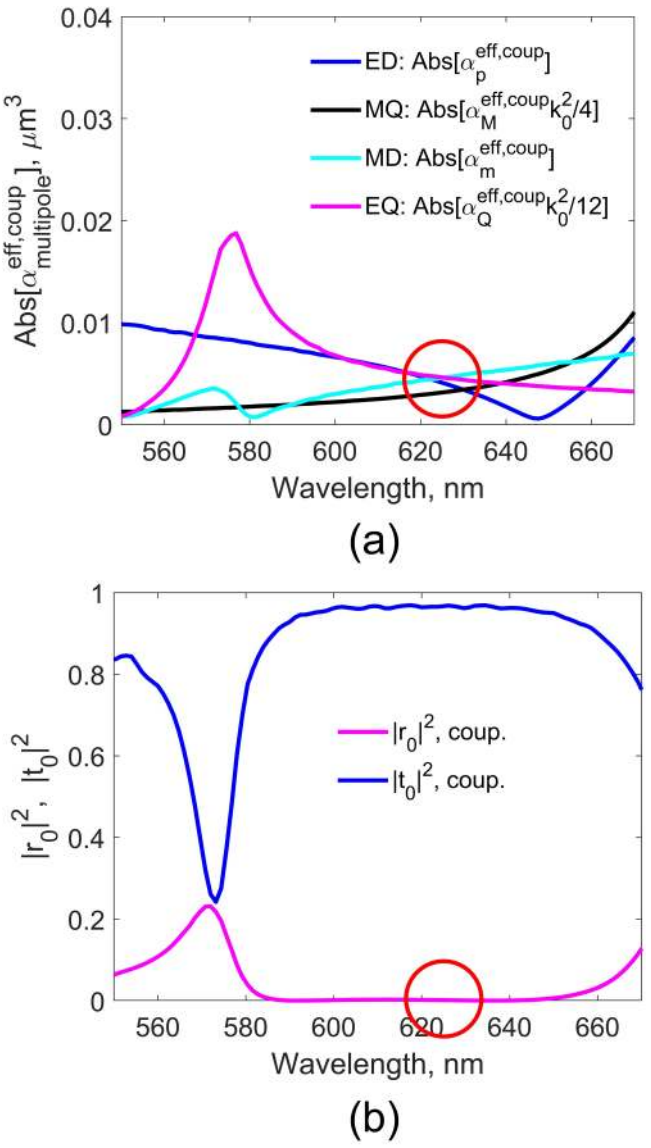

FIG. 5. (a) Absolute values of multipole terms in the expressions (43) and (44) determining the reflection and transmission coefficients, respectively, of the periodic array of spheres. (b) Intensity reflection and transmission coefficients. Red circles at the wavelength about 620–630 nm indicate the region where (i) the contributions of multipole moments in the reflection and transmission coefficients are comparable and (ii) the reflection is near zero and transmission is close to unit due to the lattice invisible (anapole) effect. The lattice periods are $D_x = 500$ nm and $D_y = 440$ nm, and silicon particles have $R = 125$ nm.

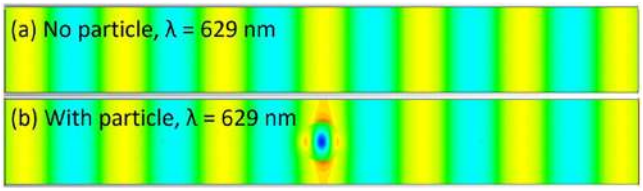

FIG. 6. Total *Ex* field distribution (incident and scattered waves) in numerical simulations of (a) and (b) a domain with a sphere in the 2D periodic array. Simulations are performed at the wavelength corresponding to the lattice anapole effect.[51]

polarizability. It can result in the induced resonant spectral features and magneto-electric response. For instance, the nanospheres of noble metals with the radius in a range of tens of nanometers appear to have only non-negligible ED polarizability of the single nanoparticle. However, the particle arrangement in the lattice results in excitation of a well-pronounced EQ collective resonance, and the latter contributes to reflection, transmission, and absorption of light in the array.[50]

Second, in the case when only one multipole in the pair ED-MQ or MD-EQ is pronounced and another is insignificant yet non-zero, the small multipole excitation can be enhanced by the counterpart. For instance, it has been shown that in the array of gold nanospheres with a radius of 100 nm, the lattice resonance is affected not only by EQ but also by lattice-induced MD (see Ref. 50). The result becomes apparent by comparing calculations that do and do not account for cross-multipole coupling with the full-wave simulations. One can see that even in the nanoparticles without a significant magnetic response, lattice resonances induce a magnetic resonance in the nanoparticle periodic arrangement.

Third, special conditions can be satisfied for effective suppression of light reflection[50] or transmission[33] from the arrays due to lattice multipole resonances. The effect concerning reflection has

	On a single scatterer	**On scatterers in the array, where positions of EDR and MDR of the scatterer are not controlled by the array periods**	**On scatterers in the array, where positions of EDR and MDR of the scatterer can be controlled by the lattice periods**
ED & MD, in phase	Kerker effect		
	First Kerker condition, Refs.[a] No backscattering; near-unit forward scattering	Refs.[b] No reflection; near-unit transmission with rapid phase change.	Lattice Kerker effect, Refs.[c] No reflection; near-unit transmission with rapid phase change
ED & MD, out of phase	anti-Kerker effect		
	Second Kerker condition, Refs.[d] No forward scattering; near-unit backscattering	Not reported	Refs.[e] Simultaneous transmission and reflection in the spectral range between EDR & MDR
Any, but most often ED & EQ, in phase	Generalized Kerker effect		
	Refs.[f] No backscattering; near-unit forward scattering	Refs.[g] No reflection; near-unit transmission with rapid phase change	Refs.[h] No reflection; near-unit transmission with rapid phase change
ED, MD, EQ, MQ Two pairs of multipoles are in phase within the pair. Pairs with respect to each other can be in-phase or out-of-phase	Invisibility (anapole) state		
	Refs.[i] Upon light incidence, neither backscattering nor forward scattering occurs from the particle.	Refs.[j] No reflection; near-unit transmission with *no phase change*	Lattice invisibility (anapole), Refs.[k] No reflection; near-unit transmission with *no phase change*

FIG. 7. Effects related to scattering directionality and lattices. The effects can occur with either non-resonant or resonant values of multipole moments. The summary concerns only multipole phase as the absolute value needs to compensate each other in magnitude. (a) Ref. 98; (b) Ref. 103; (c) Refs. 32 and 71; (d) Ref. 98; (e) Ref. 33; (f) Refs. 106 and 107; (g) Ref. 108; (h) Ref. 50; (i) Refs. 61 and 113–115; (j) Refs. 110, 112, and 116; and (k) Refs. 35, 51, and 111.

been experimentally observed in the earlier study of lattice resonances in transverse polarizations.[80] The possibility of efficient control of directional scattering, reflection, transmission, and absorption of light in the arrays with a variety of multipoles[81,82] can be applied to control light beam in metasurfaces, metalenses, perfect absorbers, and other photonic designs and light-harvesting devices.

Fourth, the resonance line shape associated with lattice resonances needs to be brought up. Fano resonances are generally defined as a resonant wave phenomenon that results in an asymmetric line shape.[73] It includes an interference between a broad, background, and narrow, resonant, process regardless of whether these resonant excitations interact (couple) or not.

Reflection and transmission spectra of a resonant Kerker effect based on ED and MD is an example of a Fano profile for non-interacting (un-coupled) resonances. The same goes for the generalized Kerker effect resulting from the compensation of ED and EQ, which are, again, uncoupled and do not affect each other. Directional scattering related to single-particle Kerker effects also has a Fano profile.[73,79]

In the plasmonic nanostructures and metamaterials, Fano resonances are often discussed in the context of interacting (coupled) resonances.[78,79] In this case, the asymmetric line shape appears not only as an interference feature in reflection and transmission spectra, but also as a modification of the resonance shape, e.g., absorption profile, stemming from excitation and coupling of two resonances. Most impressively, we observe that the cross-multipole coupling, discussed here for ED–MQ and MD–EQ pairs, results in this kind of Fano resonances. Asymmetric shapes of effective polarizabilities in Fig. 3 are examples of such Fano resonances originating from resonance coupling.[51]

The Fano profile of the lattice resonance, corresponding to a particular multipole, represents a special case of Fano resonances. Here, non-interacting multipoles facilitate a collective effect resulting in effective polarizability with an asymmetric line shape. The Fano profile of the lattice resonances arises owing to a general mechanism related to the coupling between a bright broadband mode and a narrow-band dark mode supported by a system.[73] In the periodic nanoparticle arrays, the Fano-like lattice resonances emerge due to proximity of the single-particle resonances to a diffraction edge. In this case, an evanescent diffractive wave next to the Rayleigh anomaly corresponds to the transition of diffractive order from a propagating state to an evanescent state.[74–77]

Note that the excitation of lattice resonances, leading to the appearance of narrow Fano-like resonances in the spectral characteristics of metasurfaces (see Fig. 2), can be associated with the Rayleigh anomaly of any diffraction order under the condition of appropriate resonant scattering of every particle in the lattice.[72] More generally, the lattice resonances can emerge in the proximity of Rayleigh anomaly corresponding to any arbitrary diffraction order as long as its spectral position is appropriately tuned for the Mie resonance of an isolated scatterer. However, for the wavelength shorter than the zeroth-order diffraction limit, other diffractive propagation directions are allowed. Therefore, the contribution of single-particle resonances into lattice effects associated with higher diffraction orders is assumed to be weaker.

On further studies, the addition of higher-order multipoles can result in a novel cross-multipole coupling effect providing more insight into the functional properties of metasurfaces for manipulation of light.

V. BEYOND THE NORMAL-INCIDENCE MODEL: PERIODIC GREEN FUNCTIONS

In addition to the spectral analyses of optical resonant and multipole coupling effects of metasurfaces normally irradiated by external light waves, it is possible to apply an alternative research approach based on different irradiation conditions at fixed frequencies. This consideration involves analysis in the reciprocal $(\mathbf{k}, \omega)$-space as opposed to the analytical approach in the real-coordinate space described above. The polarizability of each (isolated) spherical nanoparticle forming the metasurface depends only on the wavelength of light, and depending on irradiation condition (the incidence angle), the additional resonances are driven by collective effects providing information about multipole coupling. Using this alternative approach, the dipole–quadrupole coupling in two-dimensional arrays of spherical particles has been theoretically studied in Ref. 117. The main results have been obtained by the application of the periodic Green function technique that has been developed specifically for periodic systems with electric and magnetic dipole and quadrupole interactions.[118]

The reduction of the description of an array to a single unit cell necessitates the calculations of periodic Green functions originating from radiative interactions between unit cells. Periodic Green functions take the form of slowly convergent sums over the lattice, and acceleration techniques, such as Ewald summation, Kummer's, Poisson's, or Shank's transformation, are required to evaluate them. As has been shown in Ref. 118, one can use a generalization of an earlier approach and involve a dimensionality reduction with the Poisson transformation and a singularity removal. Considering the ED, MD, and EQ moments of each emitter, one can derive a concise analytic form for the radiative contributions to the periodic Green function dyadics that give rise to radiation reaction fields. This description of the scattered light explicitly satisfies the optical theorem, and the non-radiative contributions that do not affect energy balance in the form of a rapidly converging series are presented.

The work outlined in Ref. 117 emphasizes the importance of understanding coupling mechanisms and the link between properties of lattice resonances and the lattice mode dispersion relations in the nanoparticle arrays. Using periodic Green function dyadics allows us to analyze the connection between the modes and the resonance spectrum in detail. Using the representation of periodic Green function dyadics,[118] it is possible to clarify and investigate the sensitivity of lattice resonances to coupling and illumination conditions as well as the frequency cutoff below which lattice resonances are not found.

Importantly, the method involving periodic Green functions provides a framework for studying lattice effects under the oblique incidence of light. However, the approach is still prone to the limitation and increased complexity the same as real-coordinate space treatment. However, the extension of the approach to nanoparticles of a complex shape (other than spherical) requires consideration of tensor polarizability and can significantly complicate the derivations.

VI. BEYOND THE INFINITE MODEL: DIPOLE COUPLING IN A FINITE-SIZE ARRAY

There are a number of real-life situations where we need to study finite-size nanostructures that include nanoparticles of different sizes and/or with a disordered space distribution. The rigorous calculations of a general case of the finite-size array with different nanoparticles involve constructing a matrix equation and solving a large number of these linear equations. In the general form, the equation for ED can be presented as

$$\mathbf{p}_j = \hat{\alpha}_j \left(\mathbf{E}_0(\mathbf{r}_j) + \frac{k_0^2}{\varepsilon_0} \sum_{l \neq j}^{N} \hat{G}^p_{jl} \mathbf{p}_l + \sum_{l \neq j}^{N} \mathbf{h}^{\text{multip}}_{jl} \right), \tag{48}$$

where $j = 1, \ldots, N$, N is the number of particles in the system and vector $\mathbf{h}^{\text{multip}}_{jl}$ describes the cross-multipole coupling between ED and other multipoles (MD, EQ, MQ, etc). Similar expressions can be written for other multipoles involved into considerations.

An example of a finite-size array with the spherical nanoparticles with ED and EQ responses has been considered in Ref. 22. In this case, every particle is characterized by eight unknown variables: three independent components of a dipole moment (p_x, p_y, p_z) and five independent components of a symmetrical traceless quadrupole tensor (Q_{xx}, Q_{yy}, Q_{xy}, Q_{xz}, Q_{yz}). Thus, one can construct and solve a matrix equation, and this system of equations can be used for the analysis of arbitrarily configured systems. For a system consisting of N nanoparticles, the system required to solve has $8 \times N$ unknown variables. It has been demonstrated that with the decrease in the number of particles in the system and their polarizabilities, the resonant diffractive features in the metasurface response decrease rapidly. In the case of a nanoantenna with large polarizability (such as a relatively large plasmonic nanoparticle), results from Ref. 119 provide an insight into the characteristic length scales for collective effects: (i) for arrays smaller than 5×5 particles, the collective resonances are weak and their quality factors can be lower than those of a single nanoparticle; (ii) for arrays larger than 20×20 particles, the quality factors of collective resonances can saturate at a much larger value than those of a single nanoparticle (in this case, the resonance quality factor is basically restricted only by light absorption in the plasmonic nanostructure); and (iii) in between, the quality factors of collective resonances are an increasing function of the number of particles in the array. A similar conclusion has also been made in Ref. 120.

In the case of dielectric nanoparticles, in which the absorption can be significantly decreased, the sensitivity of the collective resonances to the finite-size parameters of nanoparticle arrays can be different. It has been recently reported in Ref. 121 that ED lattice resonances in finite-sized dielectric arrays of dielectric converge to the infinite-array model for about 50×50 nanoparticles, and MD lattice resonances in finite-sized arrays are quite different from the ones of infinite arrays even for the array with about 100×100 nanoparticles. Therefore, the use of numerical and theoretical models for infinite arrays for the estimation of finite-size structure properties needs to be separately examined for each specific case.

In addition to change of the collective resonances, the inclusion of finite-size conditions for nanoparticle arrays can facilitate cross-multipole coupling. For example, the equation system for the case of ED–MD coupling in a finite-size array can be written as[21]

$$\mathbf{p}_j = \hat{\alpha}_p \left(\mathbf{E}_0(\mathbf{r}_j) + \frac{k_0^2}{\varepsilon_0} \sum_{l \neq j}^{N} \hat{G}^p_{jl} \mathbf{p}_l + \frac{ik_S}{\varepsilon_0 \varepsilon_S c_S} \sum_{l \neq j}^{N} [\mathbf{g}_{jl} \times \mathbf{m}_l] \right), \tag{49}$$

$$\mathbf{m}_j = \hat{\alpha}_m \left(\mathbf{H}_0(\mathbf{r}_j) + k_0^2 \sum_{l \neq j}^{N} \varepsilon_S \hat{G}^p_{jl} \mathbf{m}_l - ik_S c_S \sum_{l \neq j}^{N} [\mathbf{g}_{jl} \times \mathbf{p}_l] \right), \tag{50}$$

where tensor $\hat{G}^p_{jl}$ and vector $\mathbf{g}_{jl}$ describe the interaction between dipoles and particularly, the terms containing $\mathbf{g}_{jl}$ describe cross-dipole coupling. As has been reported in Ref. 21, ED–MD cross-interactions in a finite-size array leads to excitation of the longitudinal (perpendicular to the structure plane) near-field components, values of which strongly depend on the resonances of the total array. The creation of these longitudinal electric and magnetic components arises as a boundary effect due to the finite size of the array. As a consequence, the maxima of the dipole longitudinal components are concentrated on the boundary of the structures. Examples of the spatial distributions of magnetic and electric near fields in the silicon nanoparticle arrays for the conditions of magnetic and electric diffractive resonances are shown in Figs. 8(a) and 8(b), respectively.

In most cases, the realization of nanoparticle arrays employs either a top-down (lithographic) fabrication approach with good precision of a nanoparticle position and size or a bottom-up technique with a large dispersion of sizes and little control of nanoparticle position. The developed theoretical framework and its results, shown in Ref. 122, indicate that ED and MD interactions are a key aspect in inter-particle coupling even in random arrays. The work brings an understanding of how the stochastic mutual interplay of the scattered fields in a random or amorphous array of high refractive index nanoparticles influences the array's optical properties in terms of its ED and MD resonances. Comprehensive numerical investigations of the ED and MD lattice resonances in disordered arrays of Si nanospheres have recently been reported in Ref. 123.

Future work most likely will include particles supporting higher-order multipole resonances that can significantly increase degrees of freedom for manipulations of light properties at subwavelength scales.

VII. FULL-WAVE NUMERICAL MODELING AND MULTIPOLE DECOMPOSITION

So far, we only paid attention to the metasurfaces formed by spherical nanoparticles. Naturally, there is a question: how we can extend a similar framework to the case of the metasurfaces formed by non-spherical (arbitrary) shaped nanoparticles. Below, we highlight an advanced technique to account for collective effects and multipole excitations in metasurfaces with complex-shape building blocks and flexibility in light illumination and material treatment.

For the nanoparticle where analytical or semi-analytical solutions are not available, one can apply the following procedure. First, the total electric field in nanoparticles arranged into the infinite 2D array is calculated numerically using some full-wave

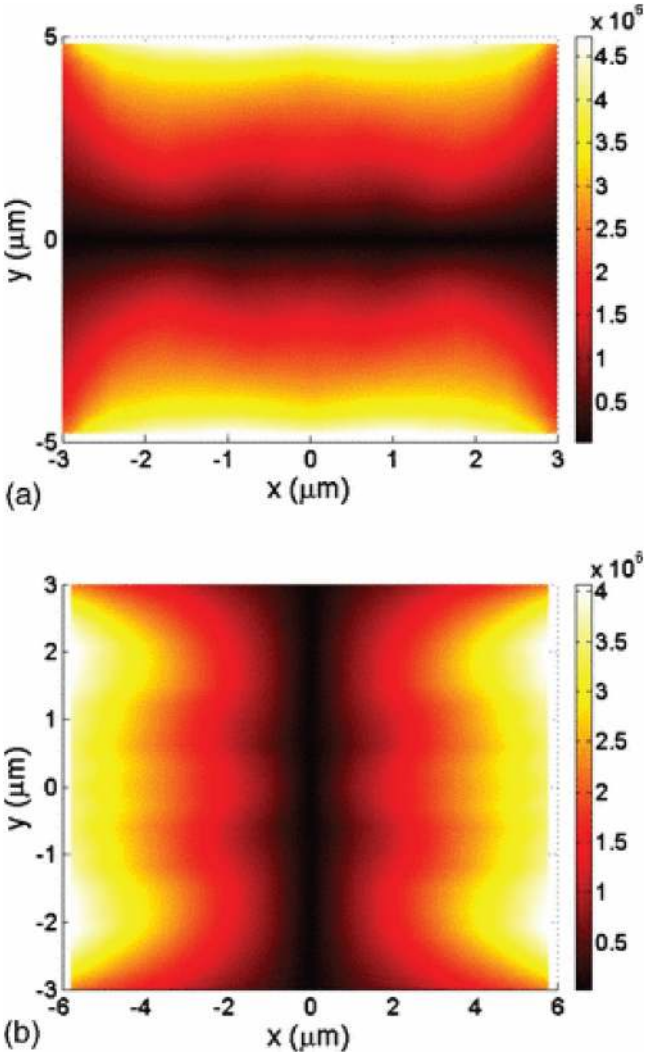

FIG. 8. The z-component field magnitudes of induced (a) MD and (b) ED (in a.u.) in periodic arrays of 21×21 nanoparticles.[21] (a) $D_x = 300$ nm, $D_y = 480$ nm—the wavelength corresponds to the global maximum of m_z. (b) $D_x = 580$ nm, $D_y = 300$ nm—the wavelength corresponds to the global maximum of p_z. Radius of the nanoparticles is 65 nm. Reproduced with permission from Evlyukhin *et al.*, Phys. Rev. B **82**, 045404 (2010). Copyright 2010 American Physical Society.

numerical simulations (for example, commercial packages COMSOL Multiphysics or CST Microwave Studio or any other implementations of a finite-difference time-domain, a finite element, or another method solving Maxwell's equations). Then, the multipole moments of the nanoparticles are calculated following their definitions presented in Ref. 57. Finally, the multipole contribution to the reflection and transmission coefficients can be estimated on the basis of the equations for the electric field reflection r and transmission t coefficients, which are written in multipole presentations. Under normal incident of light on the nanoparticle lattice, each identical nanoparticle forming an infinite periodic metasurface has the same multipole moments due to translational symmetry of the nanostructure (and periodic boundary conditions in the calculation domain). For these conditions and for x-polarized incident light (xy-plane is the metasurface plane), the r and t coefficients are[35]

$$r = \frac{ik_S}{E_0 2S_L \varepsilon_0 \varepsilon_S}\left(p_x - \frac{1}{c_S}m_y + \frac{ik_S}{6}Q_{xz} - \frac{ik_S}{2c_S}M_{yz} - \frac{k_S^2}{6}O_{xzz}\right), \tag{51}$$

$$t = 1 + \frac{ik_S}{E_0 2S_L \varepsilon_0 \varepsilon_S}\left(p_x + \frac{1}{c_S}m_y - \frac{ik_S}{6}Q_{xz} - \frac{ik_S}{2c_S}M_{yz} - \frac{k_S^2}{6}O_{xzz}\right). \tag{52}$$

For the y-polarization, the coefficients are

$$r = \frac{ik_S}{E_0 2S_L \varepsilon_0 \varepsilon_S}\left(p_y + \frac{1}{c_S}m_x + \frac{ik_S}{6}Q_{yz} + \frac{ik_S}{2c_S}M_{xz} - \frac{k_S^2}{6}O_{yzz}\right), \tag{53}$$

$$t = 1 + \frac{ik_S}{E_0 2S_L \varepsilon_0 \varepsilon_S}\left(p_y - \frac{1}{c_S}m_x - \frac{ik_S}{6}Q_{yz} + \frac{ik_S}{2c_S}M_{xz} - \frac{k_S^2}{6}O_{yzz}\right). \tag{54}$$

Here, k_S is the wave number in the surrounding medium, S_L is the area of a lattice unit cell, ε_0 is the vacuum permittivity, ε_S is the permittivity of the surrounding medium, E_0 is the electric field of the normally incident plane waves at the metasurface plane, and $c_S = 1/\sqrt{\mu_0 \varepsilon_0 \varepsilon_S}$ is the speed of light in the surrounding medium. In contrast to the cases including spherical particles, where the transmission and reflection coefficients are expressed in terms of the polarizabilities [Eqs. (43) and (44)], here, certain components of multipole moments are used. Equations (51)–(54) include contributions of several first multipoles up to the electric octupole: **p** and **m** are the vectors of ED and MD moments and $\hat{Q}$, $\hat{M}$, and $\hat{O}$ are the tensors of the EQ, MQ, and electric octupole moments, respectively. The intensity transmission and reflection coefficients are $|t|^2$ and $|r|^2$, respectively.

The method of multipole decomposition is a versatile tool to analyze the excitation of different multipoles in the nanostructure with nanoparticles of a complex shape. Another important advantage of the multipole decomposition method is a straightforward possibility to implement higher-order multipoles in the analysis of metasurface optical properties without derivation of effective multipole polarizabilities. For example, including the contribution of octupole moment can be easily done by expanding Eqs. (51)–(54) for next higher-order multipoles using a multipole representation

of scattered electric fields from Ref. 55. The number of multipoles that are enough for correct analysis can be determined from the comparison of the analytic results with numerical simulations without multipole decomposition.

While the multipole decomposition technique has flexibility in the number of multipoles included, the full-wave numerical modeling in itself provides an opportunity to analyze the structure without imposing limitations on what multipoles are considered. However, the physical interpretation of the numerically obtained results is rather difficult without multipole application.

VIII. BIANISOTROPY AND LIGHT TRAPPING WITH NANOPARTICLES OF A COMPLEX SHAPE

If the nanoparticle has an inhomogeneous internal structure or some complex shape, its optical response can include anisotropic or bianisotropic behavior. In the case of anisotropy, the induced ED or MD moment of the nanoparticle is not co-linear to the external incident field. In the case of bianisotropy, the electric (magnetic) dipole moment can be excited by both electric and magnetic fields of external incident waves.

A. Dipole coupling in metasurfaces formed by bianisotropic nanoparticles

In the case when the metasurface is formed by the nanoparticles with bianisotropic optical properties, their ED and MD moments are induced by both electric and magnetic fields in the system. In this dipole approximation, one can write[124]

$$\begin{aligned} \mathbf{p}_l &= \hat{\alpha}_l^{\mathrm{ee}}\mathbf{D}^{\mathrm{loc}}(\mathbf{r}_l) + \frac{1}{c_S}\hat{\alpha}_l^{\mathrm{em}}\mathbf{H}^{\mathrm{loc}}(\mathbf{r}_l), \\ \mathbf{m}_l &= \hat{\alpha}_l^{\mathrm{mm}}\mathbf{H}^{\mathrm{loc}}(\mathbf{r}_l) + c_S\,\hat{\alpha}_l^{\mathrm{me}}\mathbf{D}^{\mathrm{loc}}(\mathbf{r}_l), \end{aligned} \tag{55}$$

where $\mathbf{p}_l$ and $\mathbf{m}_l$ are the ED and MD moments of a particle with number l at the particle coordinate $\mathbf{r}_l$ excited by the local electric $\mathbf{E}^{\mathrm{loc}}(\mathbf{r}_l)$ and magnetic $\mathbf{H}^{\mathrm{loc}}(\mathbf{r}_l)$ fields; $\hat{\alpha}_l^{\mathrm{ee}}$, $\hat{\alpha}_l^{\mathrm{mm}}$, $\hat{\alpha}_l^{\mathrm{em}}$, and $\hat{\alpha}_l^{\mathrm{me}}$ are the electric, magnetic, electromagnetic, and magnetoelectric polarizability tensors of the particle with number l, respectively; $\mathbf{D}^{\mathrm{loc}}(\mathbf{r}_l) = \varepsilon_0\varepsilon_S\mathbf{E}^{\mathrm{loc}}(\mathbf{r}_l)$ is the local displacement field; and c_S is the light speed in the surrounding matter. The local fields are created by external waves and the dipole moments of all other nanoparticles (with number $j \neq l$) form the structure. In the case of linear constituent materials, the relation $\hat{\alpha}^{\mathrm{em}} = (-\hat{\alpha}^{\mathrm{me}})^T$ is satisfied. Note that the bianisotropic optical properties of the nanoparticles can be a result of spatially broken symmetry of their shape or internal structure.[125,126]

Due to periodicity, under normal-incidence conditions of an external electromagnetic plane wave, all nanoparticles forming the infinite array bear the same electric $\mathbf{p}$ and magnetic $\mathbf{m}$ dipole moments. However, unlike the case of isotropic metasurfaces, now nanoparticles can have dipole components perpendicular to the planes of the metasurface.[126] Excitation of these out-of-plane components is related to the magnetoelectric and electromagnetic bianisotropic polarizabilities, which are induced due to the broken in-plane symmetry of the nanoparticles. Furthermore, the out-of-plane dipole components do not collectively radiate waves in the direction perpendicular to the metasurface plane. Thus, these out-of-plane dipole components are associated with the existence of lattice trapped modes,[127–129] which are closely related to the concept of symmetry-protected bound states in the continuum (BICs).[46,130] For metasurfaces formed by isotropic lossless dipole particles, the trapped modes are their (embedded) eigenmodes that do not have a channel to light radiation. Therefore, they cannot be excited by free propagating light waves. However, the introduction of bianisotropy into particles can open a channel for the trapped mode excitation by electromagnetic plane waves normally incident on the metasurface. However, this channel also leads to the energy leakage transforming non-radiating trapped mode to the radiating, which is considered to be a quasi-trapped mode. Since the resonant excitation of the quasi-trapped modes is realized in narrow spectral intervals, this leads to the appearance of the high-quality-factor Fano resonances in the transmission and reflection spectra of all-dielectric bianisotropic metasurfaces[129] as well as the concentration of electromagnetic energy in the metasurface plane.[131] Additional analytical details of the trapped modes are discussed below. Note the experimental demonstrations and numerical results for the quasi-trapped modes excited in dielectric metasurfaces for the nonlinear and thermal processes have been recently reported.[131,132] The obtained results have convincingly demonstrated the practical importance of the system supporting the quasi-trapped mode response.

Additionally, multi-resonant bianisotropic meta-gratings, achieving efficient and directional diffraction in the mid-infrared spectral range, were recently designed and experimentally realized in Ref. 133. A metasurface formed by the all-dielectric bianisotropic particles with a broken symmetry has been fabricated and experimentally studied in the GHz frequency range as well.[134] The 2π phase change in the reflection spectrum with the value close to 1 inside the frequency range has been demonstrated.

B. Trapped modes

In the ED or MD approximation, the dipole moments of nanoparticles forming a periodic metasurface can be presented as Eq. (14) or (16). Note that in these cases, the dipole moments have only in-plane components that are determined by the polarization of normally incident external waves. Let us check a hypothetical case where all particles in the infinite array possess only dipole moment d_0 (p_0 or m_0) without any external field sources so that Eqs. (14) and (16) are reduced in general to the equation

$$(1 - \alpha_d S_d)d_0 = 0, \tag{56}$$

where α_d is the dipole polarizability and S_d is the dipole sum of a metasurface. For EDs $\alpha_d = \alpha_p/\varepsilon_0\varepsilon_S$ and $S_d = \varepsilon_S S_{pp}$, and for MDs, $\alpha_d = \alpha_m$ and $S_d = S_{mm}$. The nontrivial solution ($d_0 \neq 0$), which is called a trapped (embedded) mode, can be realized only if the following condition is satisfied:

$$\alpha_d S_d = 1. \tag{57}$$

Introducing notations $\alpha_d = \alpha' + i\alpha''$ and $S_d = S' + iS''$, where α' and S' are the real parts and α'' and S'' are the imaginary parts

of the corresponding values, Eq. (57) can be written as

$$\begin{aligned} S' &= \frac{\alpha'}{\alpha'^2+\alpha''^2} = \mathrm{Re}\frac{1}{\alpha_d}, \\ S'' &= -\frac{\alpha''}{\alpha'^2+\alpha''^2} = \mathrm{Im}\frac{1}{\alpha_d}. \end{aligned} \tag{58}$$

Outside the diffracting regime, when the periods of the particle array $D < 2\pi/k_S$, the imaginary part of the dipole sum S'' has the following value:[97,126]

$$S'' = \begin{cases} -\frac{k_S^3}{6\pi} & \text{for out-of-plane dipoles,} \\ \frac{k_S}{2S_L} - \frac{k_S^3}{6\pi} & \text{for in-plane dipoles,} \end{cases} \tag{59}$$

where S_L is the area of the array unit cell.

The general condition on the imaginary part of $1/\alpha_d$ is[96]

$$\mathrm{Im}\frac{1}{\alpha' + i\alpha''} = -\frac{\alpha''}{\alpha'^2 + \alpha''^2} \leq -\frac{k_S^3}{6\pi}. \tag{60}$$

Right- and left-hand sides of Eq. (60) are equal only in the case of lossless dipole scatterers. Comparing Eqs. (59) and (60), one can see that the second condition for S'' in Eq. (58) cannot be satisfied for metasurfaces with the in-plane dipole excitation because it is always that $S'' > \mathrm{Im}(1/\alpha_d)$ in this case.

On the other side, the condition $S'' = \mathrm{Im}(1/\alpha_d)$ can be satisfied for metasurfaces formed by lossless scatterers with the out-of-plane dipole moments oriented perpendicular to the metasurface plane. In this case, the condition of the trapped mode existence is reduced to the first equation in the system (58), which can be satisfied by tuning the lattice periodicity, as it has been demonstrated in Ref. 126. Thus, the trapped mode is an in-phase oscillation of the out-of-plane dipole moments of all particles in the metasurface. Because the out-of-plane dipoles generate only strong near fields and do not radiate collectively electromagnetic waves away from the metasurface plane into the far-field zone, the electromagnetic energy is saved and concentrated in the metasurface.

Since the trapped modes do not radiate the electromagnetic energy to the far-field zone, these trapped modes cannot be directly excited by propagating waves. However, the trapped modes can be excited in the nanostructures in some way if, for instance, the constituent building blocks are perturbed, for example, by breaking their in-plane symmetry. The example is discussed in Subsection VIII A.

Nanoparticles with complex shapes can generate more sophisticated modes. The above analysis of a bianisotropic response is limited to the dipole approximation, but it is interesting to explore the extension of the concept to a more general case of magneto-electric anisotropy of nanostructures with higher multipoles. Chiral surface lattice resonances have recently been reported in an experimental study demonstrating handedness-dependent excitations in arrays of chiral plasmonic crescents.[135]

IX. FURTHER DEVELOPMENT

The analysis of cross-multipole coupling contribution in Refs. 50 and 51 allowed the identification of the coupling role and compared the optical response of the array with and without coupling. Furthermore, extending the study to higher multipoles is needed for larger nanoparticles since the previous works have presented derivations only for ED, MD, EQ, and MQ. This Perspective mainly discusses the cases of lattices with multipole-specific and cross-multipole coupling effects for dipoles and quadrupoles of both electric and magnetic nature. Similarly, we anticipate that subsequent higher-order multipoles need to be included in the full equation system, and most likely, such theoretical models will result in the effects of cross-multipole coupling facilitated by the lattice.

It has recently been demonstrated that it is possible to realize nanoparticles with purely higher-order multipole light scattering (e.g., octopole, hexadecapole).[58] Therefore, the higher-order multipoles need to be included in the analytical and semi-analytical models of nanoparticles, starting from certain dimensions and of some materials. This requirement comes not only with the advantage of broader analysis but also with the necessity of having all multipoles at the same time. In addition to that, nanoparticles with complex shapes and consequently tensorial polarizability have to be considered in those models developed in the future.

One can capitalize on the properties of dual nanoparticles to achieve unusual optical properties for engineered nanostructures. Dual nanoparticles are those with Mie coefficients satisfying $a_n = b_n$ for $n = 1, 2, \ldots$. Recent work suggests that such dual nanoparticles can be used in metasurfaces as an alternative to dipole Huygens' metasurfaces.[112] One can substitute effective polarizabilities of the single nanoparticle from Eqs. (10) and (11) into expression for reflection coefficient r_0 [Eq. (43)]. In this case, one can see that duality condition $a_n = b_n$ always results in $r_0 = 0$. It has proven to be a challenge to realize the case of single (i.e., isolated) dual nanoparticles with natural materials. As a further development of this direction, we envision that this challenge can be overcome, and lattice contribution to effective polarizability can bring an additional degree of freedom in designing metasurfaces with required parameters.

The requirement of considering complex-shape nanoparticles, higher-order multipoles, and uncertainty in excited multipoles results in the development of multipole analysis incorporated into the full-wave numerical simulations. This technique is drastically different from all analytical and semi-analytical methods, where each multipole and their coupling can be "turned on and off" (included or excluded) whenever needed. Moreover, the multipole analysis can be applied to the arrays with complex nanoparticle structures in the elementary cells.[136] In such cases, the elementary cell can be considered a set of point multipoles determined by certain multipole polarizabilities calculated in advance.[137]

The application of multipole methods to investigate lattice electromagnetic effects is directly associated and determined by different analytical representations of the Green functions corresponding to different multipole sources. The radiative contributions to all the periodic Green function dyadics are exact and can be presented in an analytical form that identifies radiation reaction terms associated with each diffracted beam.[117,118] In turn, the non-radiative contributions are found in the form of a rapidly converging series, and they all involve summations over linear combinations of a few functions. The preliminary analysis has shown that all the singularities associated with the appearance of new diffracted orders can be

identified. Further research is needed to understand underlying mechanisms better.

One can introduce the lattice modes of dipole and multipole character to analyze the diffractive coupling. It is particularly crucial for diffractive coupling to those modes indicated by lattice resonances and accounting for energy balance in the system. Lattice modes are lossy due to both (i) absorption in the nanoparticle (non-radiative loss) and (ii) the very radiative coupling that allows access to them by incident light. With the use of the introduced representation of periodic Green function dyadics,[118] one can identify precisely the part of the coupling that leads to the radiative loss. In turn, one can also introduce the hypothetical "ideal" lattice modes by neglecting both the absorption and the radiative loss. We can understand the illumination conditions required for the lattice resonances to appear from the resulting ideal dispersion relations. Having linked lattice resonances to ideal lattice modes, one can further introduce a simplified model of the ideal lattice mode dispersion relations that explains their novel features, such as the sensitivity of lattice resonances to coupling and illumination conditions as well as the frequency cutoff below which lattice resonances are not found.

Another promising direction is to apply a nanoparticle lattice in designing large-angle diffraction metasurfaces. As mentioned above, nanoparticles of a complex shape or a combination of different nanoparticles can exhibit directional scattering due to constructive or destructive interference that can further be enhanced by arranging the nanoparticles into a lattice and bringing additional degrees of freedom to engineer the optical response. An extension of the layer-multiple-scattering method appears to be very promising for designing lattices with different types of scatterers in the unit cell.[38] Further possible investigations include rendering the layer-multiple-scattering method in engineering complex metasurfaces with large supercells, including commensurate Moiré patterns. Interesting foreseeing applications extend to efficient diffraction of light in transmission and reflection modes at large angles as well as split of an optical beam in the direction of a transmitted and reflected diffraction channel.

X. CONCLUDING REMARKS

This article of lattice effect perspectives has been devoted to discussions of multipole implementations for analysis of metasurface optical properties. A general case of nanoparticles and their array with the electric and magnetic dipole and quadrupole moments has been considered theoretically. We have highlighted an analytical model based on coupled dipole–quadrupole equations to study the optical responses of nanoparticle arrays supporting dipole and quadrupole resonances. Furthermore, we have shown how the developed model can be applied to optical properties of infinite periodic arrays of identical high refractive index spheres. We discussed how the effect of single multipole resonant transparency and a lattice Kerker effect in the nanoparticle array can be applied for efficient control of light scattering. We also showed that excitation of all dipole and quadrupole moments in the silicon nanoparticle arrays could lead to the realization of a lattice anapole state, which corresponds to a condition when particle multipoles are excited, but neither the amplitude nor the phase of the transmitted wave changes. The effects of nanoparticle coupling in finite-size structures and arrays have also been considered. The influence of finite-size parameters on the collective resonances and cross-multipole coupling has been discussed. Combined semi-analytical approaches to multipole analysis of optical properties of the metasurfaces formed by the nanoparticles of non-spherical shapes have been described in detail. Finally, for the nanoparticles of more complex shapes with broken symmetry (or introduced defect), we discussed approaches to concentrate energy in the metasurface plane due to the quasi-trapped modes' excitation.

The optical collective effects and the presented analytical, semi-analytical, and numerical techniques can be used for developing nanoparticle structures, metasurfaces, and ultra-thin photonic elements with different functional optical properties. Compared to other physical–chemical approaches to the synthesis of new materials,[138–140] the development of new artificial metamaterials and metasurfaces based on multipole resonances of their building blocks can be considered a viable alternative for expanding the material platform of modern physics research studies.

ACKNOWLEDGMENTS

This material is based upon the work supported by the Air Force Office of Scientific Research (AFOSR) under Grant No. FA9550-19-1-0032. The analysis of light trapping effects has been supported by the Russian Science Foundation (Russian Federation) (Project No. 20-12-00343). The support from the Deutsche Forschungsgemeinschaft (DFG, German Research Foundation) under Germany's Excellence Strategy within the Cluster of Excellence PhoenixD (EXC 2122, Project ID 390833453) is acknowledged.

DATA AVAILABILITY

The data that support the findings of this study are available from the corresponding author upon reasonable request.

REFERENCES

[1]L. Novotny and B. Hecht, *Principles of Nano-Optics* (Cambridge University Press, 2012).
[2]E. Prodan, C. Radloff, N. J. Halas, and P. Nordlander, "A hybridization model for the plasmon response of complex nanostructures," Science **302**, 419 (2003).
[3]T. Liu, R. Xu, P. Yu, Z. Wang, and J. Takahara, "Multipole and multimode engineering in Mie resonance-based metastructures," Nanophotonics **9**(5), 1115–1137 (2020).
[4]B. Luk'yanchuk, N. I. Zheludev, S. A. Maier, N. J. Halas, P. Nordlander, H. Giessen, and C. T. Chong, "The Fano resonance in plasmonic nanostructures and metamaterials," Nat. Mater. **9**, 707 (2010).
[5]S. V. Zhukovsky, V. E. Babicheva, A. B. Evlyukhin, I. E. Protsenko, A. V. Lavrinenko, and A. V. Uskov, "Giant photogalvanic effect in noncentrosymmetric plasmonic nanoparticles," Phys. Rev. X **4**, 031038 (2014).
[6]K. Frizyuk, M. Hasan, A. Krasnok, A. Alú, and M. Petrov, "Enhancement of Raman scattering in dielectric nanostructures with electric and magnetic Mie resonances," Phys. Rev. B **97**, 085414 (2018).
[7]A. Boulesbaa, V. E. Babicheva, K. Wang, I. I. Kravchenko, M.-W. Lin, M. Mahjouri-Samani, C. Jacob, A. A. Puretzky, K. Xiao, I. Ivanov, C. M. Rouleau, and D. B. Geohegan, "Ultrafast dynamics of metal plasmons induced by 2D semiconductor excitons in hybrid nanostructure arrays," ACS Photonics **3**, 2389 (2016).

[8]K. Frizyuk, "Second-harmonic generation in dielectric nanoparticles with different symmetries," J. Opt. Soc. Am. B **36**, F32–F37 (2019).
[9]A. Han, C. Dineen, V. E. Babicheva, and J. V. Moloney, "Second harmonic generation in metasurfaces with multipole resonant coupling," Nanophotonics **9**(11), 3545–3556 (2020).
[10]H. A. Atwater and A. Polman, "Plasmonics for improved photovoltaic devices," Nat. Mater. **9**, 205 (2010).
[11]V. E. Babicheva, R. S. Ikhsanov, S. V. Zhukovsky, I. E. Protsenko, I. V. Smetanin, and A. V. Uskov, "Hot electron photoemission from plasmonic nanostructures: The role of surface photoemission and transition absorption," ACS Photonics **2**, 1039 (2015).
[12]V. E. Babicheva, S. Gamage, M. I. Stockman, and Y. Abate, "Near-field edge fringes at sharp material boundaries," Opt. Express **25**, 23935 (2017).
[13]V. E. Babicheva, "Surface and edge resonances of phonon-polaritons in scattering near-field optical microscopy," arxiv:1709.06274 (2017).
[14]B. Lamprecht, G. Schider, R. T. Lechner, H. Ditlbacher, J. R. Krenn, A. Leitner, and F. R. Aussenegg, "Metal nanoparticle gratings: Influence of dipolar particle interaction on the plasmon resonance," Phys. Rev. Lett. **84**, 4721 (2000).
[15]S. Zou, N. Janel, and G. C. Schatz, "Silver nanoparticle array structures that produce remarkably narrow plasmon lineshapes," J. Chem. Phys. **120**, 10871 (2004).
[16]S. Zou and G. C. Schatz, "Theoretical studies of plasmon resonances in one-dimensional nanoparticle chains: Narrow lineshapes with tunable widths," Nanotechnology **17**, 2813 (2006).
[17]V. A. Markel, "Divergence of dipole sums and the nature of non-Lorentzian exponentially narrow resonances in one-dimensional periodic arrays of nanospheres," J. Phys. B: Atom. Mol. Opt. Phys. **38**, L115 (2005).
[18]V. G. Kravets, F. Schedin, and A. N. Grigorenko, "Extremely narrow plasmon resonances based on diffraction coupling of localized plasmons in arrays of metallic nanoparticles," Phys. Rev. Lett. **101**, 087403 (2008).
[19]B. Auguié and W. L. Barnes, "Collective resonances in gold nanoparticle arrays," Phys. Rev. Lett. **101**, 143902 (2008).
[20]G. Vecchi, V. Giannini, and J. Gómez Rivas, "Surface modes in plasmonic crystals induced by diffractive coupling of nanoantennas," Phys. Rev. B **80**, 201401 (2009).
[21]A. B. Evlyukhin, C. Reinhardt, A. Seidel, B. S. Luk'yanchuk, and B. N. Chichkov, "Optical response features of Si-nanoparticle arrays," Phys. Rev. B **82**, 045404 (2010).
[22]A. B. Evlyukhin, C. Reinhardt, U. Zywietz, and B. Chichkov, "Collective resonances in metal nanoparticle arrays with dipole-quadrupole interactions," Phys. Rev. B **85**, 245411 (2012).
[23]P. Offermans, M. C. Schaafsma, S. R. K. Rodriguez, Y. Zhang, M. Crego-Calama, S. H. Brongersma, and J. Gómez Rivas, "Universal scaling of the figure of merit of plasmonic sensors," ACS Nano **5**, 5151 (2011).
[24]W. Zhou, M. Dridi, J. Y. Suh, C. H. Kim, D. T. Co, M. R. Wasielewski, G. C. Schatz, and T. W. Odom, "Lasing action in strongly coupled plasmonic nanocavity arrays," Nat. Nanotechnol. **8**, 506 (2013).
[25]S. V. Zhukovsky, V. E. Babicheva, A. V. Uskov, I. E. Protsenko, and A. V. Lavrinenko, "Enhanced electron photoemission by collective lattice resonances in plasmonic nanoparticle-array photodetectors and solar cells," Plasmonics **9**, 283 (2014).
[26]S. V. Zhukovsky, V. E. Babicheva, A. V. Uskov, I. E. Protsenko, and A. V. Lavrinenko, "Electron photoemission in plasmonic nanoparticle arrays: Analysis of collective resonances and embedding effects," Appl. Phys. A **116**, 929 (2014).
[27]B. D. Thackray, P. A. Thomas, G. H. Auton, F. J. Rodriguez, O. P. Marshall, V. G. Kravets, and A. N. Grigorenko, "Super-narrow, extremely high quality collective plasmon resonances at telecom wavelengths and their application in a hybrid graphene-plasmonic modulator," Nano Lett. **15**, 3519 (2015).
[28]V. Babicheva, I. Staude, and D. Gerard, "Collective effects and coupling phenomena in resonant optical metasurfaces: Introduction," J. Opt. Soc. Am. B **36**(7), CEC1–CEC3 (2019).
[29]S. Murai, G. W. Castellanos, T. V. Raziman, A, G. Curto, and J. Gomez Rivas, "Enhanced light emission by magnetic and electric resonances in dielectric metasurfaces," Adv. Opt. Mater. **8**, 1902024 (2020).
[30]G. W. Castellanos, P. Bai, and J. Gómez Rivas, "Lattice resonances in dielectric metasurfaces," J. Appl. Phys. **125**, 213105 (2019).
[31]J. Li, N. Verellen, and P. Van Dorpe, "Engineering electric and magnetic dipole coupling in arrays of dielectric nanoparticles," J. Appl. Phys. **123**, 083101 (2018).
[32]V. E. Babicheva and A. B. Evlyukhin, "Resonant lattice Kerker effect in metasurfaces with electric and magnetic optical responses," Laser Photonics Rev. **11**, 1700132 (2017).
[33]V. E. Babicheva and A. B. Evlyukhin, "Resonant suppression of light transmission in high-refractive-index nanoparticle metasurfaces," Opt. Lett. **43**, 5186–5189 (2018).
[34]A. B. Evlyukhin, M. Matiushechkina, V. A. Zenin, M. Heurs, and B. N. Chichkov, "Lightweight metasurface mirror of silicon nanospheres," Opt. Mat. Express **10**, 2706–2716 (2020).
[35]P. D. Terekhov, V. E. Babicheva, K. V. Baryshnikova, A. S. Shalin, A. Karabchevsky, and A. B. Evlyukhin, "Multipole analysis of dielectric metasurfaces composed of nonspherical nanoparticles and lattice invisibility effect," Phys. Rev. B **99**, 045424 (2019).
[36]W. Liu and Y. S. Kivshar, "Multipolar interference effects in nanophotonics," Philos. Trans. R. Soc. A **375**, 20160317 (2017).
[37]M. Q. Liu and C. Y. Zhao, "Reconfigurable metalattices: Combining multipolar lattice resonances and magneto-optical effect in far and near fields," J. Appl. Phys. **126**, 113105 (2019).
[38]E. Panagiotidis, E. Almpanis, N. Stefanou, and N. Papanikolaou, "Multipolar interactions in Si sphere metagratings," J. Appl. Phys. **128**, 093103 (2020).
[39]E. Popov, L. Mashev, and D. Maystre, "Theoretical study of the anomalies of coated dielectric gratings," Opt. Acta Int. J. Opt. **33**(5), 607–619 (1986).
[40]V. G. Kravets, A. V. Kabashin, W. L. Barnes, and A. N. Grigorenko, "Plasmonic surface lattice resonances: A review of properties and applications," Chem. Rev. **118**, 5912–5951 (2018).
[41]W. Wang, M. Ramezani, A. I. Väkeväinen, P. Törmä, J. Gómez Rivas, and T. W. Odom, "The rich photonic world of plasmonic nanoparticle arrays," Mater. Today **21**, 303 (2018).
[42]S. Baur, S. Sanders, and A. Manjavacas, "Hybridization of lattice resonances," ACS Nano **12**, 1618–1629 (2018).
[43]J. M. MacLaren, S. Crampin, D. D. Yvedensky, R. C. Albers, and J. B. Pendry, "Layer Korringa-Kohn-Rostoker electronic structure code for bulk and interface geometries," Comput. Phys. Commun. **60**, 365–389 (1990).
[44]N. Stefanou, V. Yannopapas, and A. Modinos, "MULTEM 2: A new version of the program for transmission and band-structure calculations of photonic crystals," Comput. Phys. Commun. **132**, 189–196 (2000).
[45]M. Nečada and P. Törmä, "Multiple-scattering T-matrix simulations for nanophotonics: Symmetries and periodic lattices," arXiv:2006.12968 (2020).
[46]K. Koshelev, S. Lepeshov, M. Liu, A. Bogdanov, and Y. Kivshar, "Asymmetric metasurfaces with high-Q resonances governed by bound states in the continuum," Phys. Rev. Lett. **121**, 193903 (2018).
[47]K. Fan, J. Zhang, X. Liu, G.-F. Zhang, R. D. Averitt, and W. J. Padilla, "Phototunable dielectric Huygens' metasurfaces," Adv. Mater. **30**, 1800278 (2018).
[48]Z. Sadrieva, K. Frizyuk, M. Petrov, Y. Kivshar, and A. Bogdanov, "Multipolar origin of bound states in the continuum," Phys. Rev. B **100**, 115303 (2019).
[49]S. Gladyshev, K. Frizyuk, and A. Bogdanov, "Symmetry analysis and multipole classification of eigenmodes in electromagnetic resonators for engineering their optical properties," Phys. Rev. B **102**, 075103 (2020).
[50]V. E. Babicheva and A. B. Evlyukhin, "Metasurfaces with electric quadrupole and magnetic dipole resonant coupling," ACS Photonics **5**, 2022 (2018).
[51]V. E. Babicheva and A. B. Evlyukhin, "Analytical model of resonant electromagnetic dipole-quadrupole coupling in nanoparticle arrays," Phys. Rev. B **99**, 195444 (2019).
[52]V. E. Babicheva and A. B. Evlyukhin, "Interplay and coupling of electric and magnetic multipole resonances in plasmonic nanoparticle lattices," MRS Commun. **8**, 712–717 (2018).

[53]C. H. Papas, *Theory of Electromagnetic Wave Propagation* (Dover, 1988).
[54]A. B. Evlyukhin, C. Reinhardt, E. Evlyukhin, and B. N. Chichkov, "Multipole analysis of light scattering by arbitrary-shaped nanoparticles on a plane surface," J. Opt. Soc. Am. B **30**, 2589 (2013).
[55]A. B. Evlyukhin and B. N. Chichkov, "Multipole decompositions for directional light scattering," Phys. Rev. B **100**, 125415 (2019).
[56]A. B. Evlyukhin, T. Fischer, C. Reinhardt, and B. N. Chichkov, "Optical theorem and multipole scattering of light by arbitrarily shaped nanoparticles," Phys. Rev. B **94**, 205434 (2016).
[57]R. Alaee, C. Rockstuhl, and I. Fernandez-Corbaton, "An electromagnetic multipole expansion beyond the long-wavelength approximation," Opt. Commun. **407**, 17–21 (2018).
[58]V. A. Zenin, C. E. Garcia-Ortiz, A. B. Evlyukhin, Y. Yang, R. Malureanu, S. M. Novikov, V. Coello, B. N. Chichkov, S. I. Bozhevolnyi, A. V. Lavrinenko, and N. A. Mortensen, "Engineering nanoparticles with pure high-order multipole scattering," ACS Photonics **7**, 1067–1075 (2020).
[59]J. D. Jackson, *Classical Electrodynamics* (Wiley, New York, 1999).
[60]N. Papasimakis, V. A. Fedotov, V. Savinov, T. A. Raybould, and N. I. Zheludev, "Electromagnetic toroidal excitations in matter and free space," Nat. Mater. **15**, 263–271 (2016).
[61]Y. Yang and S. I. Bozhevolnyi, "Nonradiating anapole states in nanophotonics: From fundamentals to applications," Nanotechnology **30**, 204001 (2019).
[62]R. Alaee, C. Rockstuhl, and I. Fernandez-Corbaton, "Exact multipolar decompositions with applications in nanophotonics," Adv. Opt. Mater. **7**, 1800783 (2018).
[63]R. Colom, R. McPhedran, B. Stout, and N. Bonod, "Modal expansion of the scattered field: Causality, nondivergence, and nonresonant contribution," Phys. Rev. B **98**(8), 085418 (2018).
[64]C. F. Bohren and D. R. Huffman, *Absorption and Scattering of Light by Small Particles* (Wiley Interscience, New York, 1983).
[65]V. M. Dubovik and V. V. Tugushev, "Toroid moments in electrodynamics and solid-state physics," Phys. Rep. **187**, 145–202 (1990).
[66]E. A. Gurvitz, K. S. Ladutenko, P. A. Dergachev, A. B. Evlyukhin, A. E. Miroshnichenko, and A. S. Shalin, "The high-order toroidal moments and anapole states in all-dielectric photonics," Laser Photonics Rev. **13**, 1800266 (2019).
[67]J. A. Schuller and M. L. Brongersma, "General properties of dielectric optical antennas," Opt. Express **17**, 24084 (2009).
[68]V. Babicheva, M. Petrov, K. Baryshnikova, and P. Belov, "Reflection compensation mediated by electric and magnetic resonances of all-dielectric metasurfaces [Invited]," J. Opt. Soc. Am. B **34**, D18 (2017).
[69]K. V. Baryshnikova, M. I. Petrov, V. E. Babicheva, and P. A. Belov, "Plasmonic and silicon spherical nanoparticle antireflective coatings," Sci. Rep. **6**, 22136 (2016).
[70]P. D. Terekhov, K. V. Baryshnikova, Y. A. Artemyev, A. Karabchevsky, A. S. Shalin, and A. B. Evlyukhin, "Multipolar response of nonspherical silicon nanoparticles in the visible and near-infrared spectral ranges," Phys. Rev. B **96**, 035443 (2017).
[71]C.-Y. Yang, J.-H. Yang, Z.-Y. Yang, Z.-X. Zhou, M.-G. Sun, V. E. Babicheva, and K.-P. Chen, "Nonradiating silicon nanoantenna metasurfaces as narrowband absorbers," ACS Photonics **5**, 2596 (2018).
[72]A. D. Utyushev, V. I. Zakomirnyi, A. E. Ershov, V. S. Gerasimov, S. V. Karpov, and I. L. Rasskazov, "Collective lattice resonances in all-dielectric nanostructures under oblique incidence," Photonics **7**, 24 (2020).
[73]A. E. Miroshnichenko, S. Flach, and Y. S. Kivshar, "Fano resonances in nanoscale structures," Rev. Mod. Phys. **82**, 2257 (2010).
[74]S. R. K. Rodriguez, A. Abass, B. Maes, O. T. A. Janssen, G. Vecchi, and J. Gómez Rivas, "Coupling bright and dark plasmonic lattice resonances," Phys. Rev. X **1**, 021019 (2011).
[75]M. Kataja, T. K. Hakala, A. Julku, M. J. Huttunen, S. van Dijken, and P. Törmä, "Surface lattice resonances and magneto-optical response in magnetic nanoparticle arrays," Nat. Commun. **6**, 7072 (2015).
[76]W. Zhao and Y. Jiang, "Experimental demonstration of sharp Fano resonance within binary gold nanodisk array through lattice coupling effects," Opt. Lett. **40**, 93–96 (2015).
[77]Y. Huang, L. Ma, M. Hou, and Z. Zhang, "Universal near-field interference patterns of Fano resonances in two-dimensional plasmonic crystals," Plasmonics **11**, 1377–1383 (2016).
[78]A. Lovera, B. Gallinet, P. Nordlander, and O. J. F. Martin, "Mechanisms of Fano resonances in coupled plasmonic systems," ACS Nano **7**, 4527–4536 (2013).
[79]B. Luk'yanchuk, N. Zheludev, S. Maier *et al.*, "The Fano resonance in plasmonic nanostructures and metamaterials," Nat. Mater. **9**, 707–715 (2010).
[80]A. G. Nikitin, "Diffraction-induced subradiant transverse-magnetic lattice plasmon modes in metal nanoparticle arrays," Appl. Phys. Lett. **104**, 061107 (2014).
[81]V. E. Babicheva, "Multipole resonances and directional scattering by hyperbolic-media antennas," arXiv:1706.07259 (2017).
[82]V. E. Babicheva, "Directional scattering by the hyperbolic-medium antennas and silicon particles," MRS Adv. **3**, 1913 (2018).
[83]C. M. Linton, "Lattice sums for the Helmholtz equation," SIAM Rev. **52**, 630–674 (2010).
[84]A. Moroz, "Quasi-periodic Green's functions of the Helmholtz and Laplace equations," J. Phys. A: Math. Gen. **39**, 11247–11282 (2006).
[85]P. P. Ewald, "Die Berechnung optischer und elektrostatischer Gitterpotentiale," Ann. Phys. **369**, 253 (1921).
[86]M. L. Glasser and I. J. Zucker, "Lattice sums," in *Theoretical Chemistry: Advances and Perspectives*, edited by H. Eyring and D. Henderson (Academic, New York, 1980), Vol. 5, pp. 67–139.
[87]P. A. Belov and C. R. Simovski, "Homogenization of electromagnetic crystals formed by uniaxial resonant scatterers," Phys. Rev. E **72**, 026615 (2005).
[88]P. Lunnemann, I. Sersic, and A. F. Koenderink, "Optical properties of two-dimensional magnetoelectric point scattering lattices," Phys. Rev. B **88**, 245109 (2013).
[89]B. Stout and R. McPhedran, "Electromagnetic response of chains of spheres: Dynamics to quasi-statics," Wave Motion **70**, 29–46 (2017).
[90]Y. Chen, Y. Zhang, and A. F. Koenderink, "General point dipole theory for periodic metasurfaces: Magnetoelectric scattering lattices coupled to planar photonic structures," Opt. Express **25**, 21358–21378 (2017).
[91]I. M. Fradkin, S. A. Dyakov, and N. A. Gippius, "Fourier modal method for the description of nanoparticle lattices in the dipole approximation," Phys. Rev. B **99**, 075310 (2019).
[92]A. M. Ozorio de Almeida, "Real-space methods for interpreting electron micrograph in cross-grating orientations. I. Exact wave-mechanical formulation," Acta Crystallogr. Sect. A: Found. Adv. **31**(4), 435–442 (1975).
[93]M. V. Berry, "Quantizing a classically ergodic system: Sinai's billiard and the KKR method," Ann. Phys. **131**(1), 163–216 (1981).
[94]N. Stefanou, V. Yannopapas, and A. Modinos, "Heterostructures of photonic crystals: Frequency bands and transmission coefficients," Comput. Phys. Commun. **113**(1), 49–77 (1998).
[95]E. Palik, *Handbook of Optical Constant of Solids* (Academic, San Diego, CA, 1985).
[96]A. Alù and N. Engheta, "Theory of linear chains of metamaterial/plasmonic particles as subdiffraction optical nanotransmission lines," Phys. Rev. B **74**, 205436 (2006).
[97]F. J. García de Abajo, "Colloquium: Light scattering by particle and hole arrays," Rev. Mod. Phys. **79**, 1267 (2007).
[98]M. Kerker, D. Wang, and C. Giles, "Electromagnetic scattering by magnetic spheres," J. Opt. Soc. Am. **73**, 765 (1983).
[99]Y. H. Fu, A. I. Kuznetsov, A. E. Miroshnichenko, Y. F. Yu, and B. Lukyanchuk, "Directional visible light scattering by silicon nanoparticles," Nat. Commun. **4**, 1527 (2013).
[100]S. Person, M. Jain, Z. Lapin, J. J. Sáenz, G. Wicks, and L. Novotny, "Demonstration of zero optical backscattering from single nanoparticles," Nano Lett. **13**(4), 1806–1809 (2013).
[101]J. van de Groep and A. Polman, "Designing dielectric resonators on substrates: Combining magnetic and electric resonances," Opt. Express **21**, 26285–26302 (2013).

[102]A. B. Evlyukhin, C. Reinhardt, and B. N. Chichkov, "Multipole light scattering by nonspherical nanoparticles in the discrete dipole approximation," Phys. Rev. B **84**, 235429 (2011).
[103]I. Staude, A. E. Miroshnichenko, M. Decker, N. T. Fofang, S. Liu, E. Gonzales, J. Dominguez, T. S. Luk, D. N. Neshev, I. Brener, and Y. Kivshar, "Tailoring directional scattering through magnetic and electric resonances in subwavelength silicon nanodisks," ACS Nano **7**, 7824–7832 (2013).
[104]M. Decker, I. Staude, M. Falkner, J. Dominguez, D. N. Neshev, I. Brener, T. Pertsch, and Y. S. Kivshar, "High-efficiency dielectric Huygens surfaces," Adv. Opt. Mater. **3**, 813–820 (2015).
[105]D. Sikdar, W. Cheng, and M. Premaratne, "Optically resonant magneto-electric cubic nanoantennas for ultra-directional light scattering," J. Appl. Phys. **117**, 083101 (2015).
[106]W. Liu and Y. S. Kivshar, "Generalized Kerker effects in nanophotonics and meta-optics [Invited]," Opt. Express **26**, 13085–13105 (2018).
[107]R. Alaee, R. Filter, D. Lehr, F. Lederer, and C. Rockstuhl, "A generalized Kerker condition for highly directive nanoantennas," Opt. Lett. **40**, 2645–2648 (2015).
[108]A. Pors, S. K. H. Andersen, and S. I. Bozhevolnyi, "Unidirectional scattering by nanoparticles near substrates: Generalized Kerker conditions," Opt. Express **23**, 28808–28828 (2015).
[109]Y. Yang, A. E. Miroshnichenko, S. V. Kostinski, M. Odit, P. Kapitanova, M. Qiu, and Y. S. Kivshar, "Multimode directionality in all-dielectric metasurfaces," Phys. Rev. B **95**, 165426 (2017).
[110]H. K. Shamkhi, K. V. Baryshnikova, A. Sayanskiy, P. Kapitanova, P. D. Terekhov, P. Belov, A. Karabchevsky, A. B. Evlyukhin, Y. Kivshar, and A. S. Shalin, "Transverse scattering and generalized Kerker effects in all-dielectric Mie-resonant metaoptics," Phys. Rev. Lett. **122**, 193905 (2019).
[111]H. K. Shamkhi, A. Sayanskiy, A. C. Valero, A. S. Kupriianov, P. Kapitanova, Y. S. Kivshar, A. S. Shalin, and V. R. Tuz, "Transparency and perfect absorption of all-dielectric resonant metasurfaces governed by the transverse Kerker effect," Phys. Rev. Mater. **3**, 085201 (2019).
[112]A. Rahimzadegan, D. Arslan, D. Dams, A. Groner, X. Garcia-Santiago, R. Alaee, I. Fernandez-Corbaton, T. Pertsch, I. Staude, and C. Rockstuhl, "Beyond dipolar Huygens' metasurfaces for full-phase coverage and unity transmittance," Nanophotonics **9**, 75–82 (2020).
[113]A. E. Miroshnichenko, A. B. Evlyukhin, Y. F. Yu, R. M. Bakker, A. Chipouline, A. I. Kuznetsov, B. Luk'yanchuk, B. N. Chichkov, and Y. S. Kivshar, "Nonradiating anapole modes in dielectric nanoparticles," Nat. Commun. **6**, 8069 (2015).
[114]K. V. Baryshnikova, D. A. Smirnova, B. S. Luk'yanchuk, and Y. S. Kivshar, "Optical anapoles: Concepts and applications," Adv. Opt. Mater. **7**, 1801350 (2019).
[115]R. Colom, R. McPhedran, B. Stout, and N. Bonod, "Modal analysis of anapoles, internal fields, and Fano resonances in dielectric particles," J. Opt. Soc. Am. B **36**, 2052–2061 (2019).
[116]A. K. Ospanova, I. V. Stenishchev, and A. A. Basharin, "Anapole mode sustaining silicon metamaterials in visible spectral range," Laser Photonics Rev. **12**, 1800005 (2018).
[117]S. D. Swiecicki and J. E. Sipe, "Surface-lattice resonances in two-dimensional arrays of spheres: Multipolar interactions and a mode analysis," Phys. Rev. B **95**, 195406 (2017).
[118]S. D. Swiecicki and J. E. Sipe, "Periodic Green functions for 2D magnetoelectric quadrupolar arrays: Explicitly satisfying the optical theorem," J. Opt. **19**, 095006 (2017).
[119]S. R. K. Rodriguez, M. C. Schaafsma, A. Berrier, and J. Gómez Rivas, "Collective resonances in plasmonic crystals: Size matters," Physica B **407**, 4081–4085 (2012).
[120]L. Zundel and A. Manjavacas, "Finite-size effects on periodic arrays of nanostructures," J. Phys.: Photonics **1**, 015004 (2019).
[121]V. I. Zakomirnyi, A. E. Ershov, V. S. Gerasimov, S. V. Karpov, H. Ågren, and I. L. Rasskazov, "Collective lattice resonances in arrays of dielectric nanoparticles: A matter of size," Opt. Lett. **44**, 5743–5746 (2019).
[122]K. M. Czajkowski and T. J. Antosiewicz, "Electromagnetic coupling in optical devices based on random arrays of dielectric nanoresonators," J. Phys. Chem. C **124**, 896–905 (2020).
[123]V. I. Zakomirnyi, S. V. Karpov, H. Ågren, and I. L. Rasskazov, "Collective lattice resonances in disordered and quasi-random all-dielectric metasurfaces," J. Opt. Soc. Am. B **36**, E21–E29 (2019).
[124]V. S. Asadchy, A. Díaz-Rubio, and S. A. Tretyakov, "Bianisotropic metasurfaces: Physics and applications," Nanophotonics **7**, 1069 (2018).
[125]R. Alaee, M. Albooyeh, A. Rahimzadegan, M. S. Mirmoosa, Y. S. Kivshar, and C. Rockstuhl, "All-dielectric reciprocal bianisotropic nanoparticles," Phys. Rev. B **92**, 245130 (2015).
[126]A. B. Evlyukhin, V. R. Tuz, V. S. Volkov, and B. N. Chichkov, "Bianisotropy for light trapping in all-dielectric metasurfaces," Phys. Rev. B **101**, 205415 (2020).
[127]V. A. Fedotov, M. Rose, S. L. Prosvirnin, N. Papasimakis, and N. I. Zheludev, "Sharp trapped-mode resonances in planar metamaterials with a broken structural symmetry," Phys. Rev. Lett. **99**, 147401 (2007).
[128]V. V. Khardikov, E. O. Iarko, and S. L. Prosvirnin, "A giant red shift and enhancement of the light confinement in a planar array of dielectric bars," J. Opt. **14**, 035103 (2012).
[129]V. R. Tuz, V. V. Khardikov, A. S. Kupriianov, K. L. Domina, S. Xu, H. Wang, and H.-B. Sun, "High-quality trapped modes in all-dielectric metamaterials," Opt. Express **26**, 2905 (2018).
[130]C. W. Hsu, B. Zhen, A. D. Stone, J. D. Joannopoulos, and M. Soljacic, "Bound states in the continuum," Nat. Rev. Mater. **1**, 16048 (2016).
[131]L. Xu, K. Zangeneh Kamali, L. Huang, M. Rahmani, A. Smirnov, R. Camacho-Morales, Y. Ma, G. Zhang, M. Woolley, D. Neshev, and A. E. Miroshnichenko, "Dynamic nonlinear image tuning through magnetic dipole quasi-BIC ultrathin resonators," Adv. Sci. **6**, 1802119 (2019).
[132]K. Z. Kamali, L. Xu, J. Ward, K. Wang, G. Li, A. E. Miroshnichenko, D. Neshev, and M. Rahmani, "Reversible image contrast manipulation with thermally tunable dielectric metasurfaces," Small **15**, 1805142 (2019).
[133]Z. Fan, M. R. Shcherbakov, M. Allen, J. Allen, B. Wenner, and G. Shvets, "Perfect diffraction with multiresonant bianisotropic metagratings," ACS Photonics **5**, 4303–4311 (2018).
[134]M. Odit, P. Kapitanova, P. Belov, R. Alaee, C. Rockstuhl, and Y. S. Kivshar, "Experimental realisation of all-dielectric bianisotropic metasurfaces," Appl. Phys. Lett. **108**, 221903 (2016).
[135]E. S. A. Goerlitzer, R. Mohammadi, S. Nechayev, K. Volk, M. Rey, P. Banzer, M. Karg, and N. Vogel, "Chiral surface lattice resonances," Adv. Mater. **32**, 2001330 (2020).
[136]V. R. Tuz, V. Dmitriev, and A. B. Evlyukhin, "Antitoroidic and toroidic orders in all-dielectric metasurfaces for optical near-field manipulation," ACS Appl. Nano Mater. **3**, 11315–11325 (2020).
[137]J. Mun, S. So, J. Jang, and J. Rho, "Describing meta-atoms using the exact higher-order polarizability tensors," ACS Photonics **7**, 1153–1162 (2020).
[138]E. Evlyukhin, E. Kim, D. Goldberger, P. Cifligu, S. Schyck, P. F. Weck, and M. Pravica, "High-pressure-assisted X-ray-induced damage as a new route for chemical and structural synthesis," Phys. Chem. Chem. Phys. **20**, 18949–18956 (2018).
[139]Y. Sun, Z. Liu, P. Pianetta, and D.-I. Lee, "Formation of cesium peroxide and cesium superoxide on InP photocathode activated by cesium and oxygen," J. Appl. Phys. **102**, 074908 (2007).
[140]E. Evlyukhin, E. Kim, P. Cifligu, D. Goldberger, S. Schyck, B. Harris, S. Torres, G. R. Rossman, and M. Pravica, "Synthesis of a novel strontium-based wide-bandgap semiconductor via X-ray photochemistry at extreme conditions," J. Mater. Chem. C **6**, 12473–12478 (2018).